Molecular Pharmacology Fast Forward. Published on February 1, 2011 as doi:10.1124/mol.110.070086

A Mechanistic and Structural Analysis of the Inhibition of Heat Shock Protein 90 by the Benzoquinone and Hydroquinone Ansamycins

Philip Reigan, David Siegel, Wenchang Guo, and David Ross

Department of Pharmaceutical Sciences, School of Pharmacy, University of Colorado Denver, Denver, Colorado 80045, USA.

Molecular Pharmacology Fast Forward. Published on February 1, 2011 as DOI: 10.1124/mol.110.070086
This article has not been copyedited and formatted. The final version may differ from this version.

Running Title: Hsp90 Inhibition by benzoquinone and hydroquinone ansamycins

To whom correspondence should be addressed:

David Ross

Department of Pharmaceutical Sciences,

C238-P15, Research 2,

12700 East 19th Avenue, Room 3100,

Aurora, Colorado 80045 USA

e-mail: david.ross@ucdenver.edu

Tel: 303-724-7265

Fax: 303-724-7266

Number of text pages: 21

Number of tables: 3

Number of schemes: 2

Number of figures: 5

Number of references: 41

Number of words in Abstract: 243

Number of words in Introduction: 719

Number of words in Discussion: 1365

Molecular Pharmacology Fast Forward. Published on February 1, 2011 as DOI: 10.1124/mol.110.070086
This article has not been copyedited and formatted. The final version may differ from this version.

Abbreviations: 17AAG, 17-(allylamino)-17-demethoxygeldanamycin; 17AAGH_2, 17-(allylamino)-17-demethoxygeldanamycin hydroquinone; 17AG, 17-(amino)-17-demethoxygeldanamycin; 17AGH_2, 17-(amino)-17-demethoxygeldanamycin hydroquinone; BSA, bovine serum albumin; CVFF, consistent valence forcefield; DCPIP, 2,6-dichlorophenol-indophenol; 17DMAG, 17-demethoxy-17-[[2-(dimethylamino)ethyl]amino]-geldanamycin; 17DMAGH_2, 17-demethoxy-17-[[2-(dimethylamino)ethyl]amino]-geldanamycin hydroquinone; 17AEP-GA, 17-demethoxy-17-[[2-(pyrrolidin-1-yl)ethyl]amino]-geldanamycin; 17AEP-GAH_2, 17-demethoxy-17-[[2-(pyrrolidin-1-yl)ethyl]amino]-geldanamycin hydroquinone; ES936, 5-methoxy-1,2-dimethyl-3-[(4-nitrophenoxy)methyl]indole-4,7-dione; GM, geldanamycin; GMH_2, geldanamycin hydroquinone; Hsp90, heat shock protein 90; NQO1, NAD(P)H:quinone oxidoreductase 1; PDB, Protein Data Bank; RCSB, Research Collaboratory for Structural Bioinformatics.

Molecular Pharmacology Fast Forward. Published on February 1, 2011 as DOI: 10.1124/mol.110.070086
This article has not been copyedited and formatted. The final version may differ from this version.

Abstract

The benzoquinone ansamycins inhibit the ATPase activity of heat shock protein 90 (Hsp90), disrupting the function of numerous client proteins involved in oncogenesis. In this study we examine the role of NAD(P)H:quinone oxidoreductase 1 (NQO1) in the metabolism of *trans*- and *cis*-amide isomers of the benzoquinone ansamycins and their mechanism of Hsp90 inhibition. Inhibition of purified human Hsp90 by a series of benzoquinone ansamycins was examined in the presence and absence of NQO1, and their relative rate of NQO1-mediated reduction was determined. Computational-based molecular docking simulations indicated that the *trans*- but not the *cis*- amide isomers of the benzoquinone ansamycins could be accommodated by the NQO1 active site, and the ranking order of binding energies correlated with the relative reduction rate using purified human NQO1. The *trans*-*cis* isomerization of the benzoquinone ansamycins in Hsp90 inhibition has been disputed in recent reports. Previous computational studies have used the closed or co-crystallized Hsp90 structures in an attempt to explore this isomerization step; however, we have successfully docked both the *trans*- and *cis*-amide isomers of the benzoquinone ansamycins into the open Hsp90 structure. The results of these studies indicate that both *trans*- and *cis*-amide isomers of the hydroquinone ansamycins exhibited increased binding affinity for Hsp90 relative to their parent quinones. Our data supports a mechanism where *trans*- rather than *cis*-amide forms of benzoquinone ansamycins are metabolized by NQO1 to hydroquinone ansamycins and that Hsp90-mediated *trans*-*cis* isomerization via tautomerization plays an important role in subsequent Hsp90 inhibition.

Molecular Pharmacology Fast Forward. Published on February 1, 2011 as DOI: 10.1124/mol.110.070086
This article has not been copyedited and formatted. The final version may differ from this version.

Introduction

Heat shock protein 90 (Hsp90) is overexpressed in cancer cells and implicated in their survival by maintaining the active conformation of key oncogenic proteins, including ErbB2, Raf-1, Akt, HIF-1α, and mutant p53 (Maloney and Workman, 2002). The function of Hsp90 is complex and involves homodimerization, recruitment of co-chaperones, accessory proteins, and the client protein, operating in a dynamic "chaperone cycle" dependent on the ATPase activity of Hsp90 (Pearl and Prodromou, 2006). Hsp90 is an important anticancer target and the conserved ATP-binding domain of Hsp90 is also the binding site of the natural products geldanamycin (GM) and radicicol, and a range of semi-synthetic and synthetic compounds (Roe et al., 1999; Maloney and Workman, 2002). These compounds prevent Hsp90 from cycling between ADP- and ATP-bound conformations, resulting in the degradation of multiple oncogenic client proteins via the ubiquitin-proteasome pathway and ultimately growth arrest or apoptosis (Maloney and Workman, 2002).

The benzoquinone ansamycin class of Hsp90 inhibitors include GM and its semi-synthetic derivative 17-allylamino-17-demethoxy-geldanamycin (17AAG), which have been shown to bind to Hsp90 with micromolar affinity *in vitro* and with nanomolar activity *in vivo* (Roe et al., 1999; Chiosis et al., 2003), and have demonstrated selectivity towards tumor cells (Chiosis and Neckers, 2006). The benzoquinone ansamycins exist in two isomeric forms, in solution they adopt an almost planar *trans*-amide conformation (Schnur and Corman, 1994), while co-crystallization studies indicate the formation of the C-shaped *cis*-amide isomer in the nucleotide-binding site of Hsp90 (Stebbins et al., 1997; Jez et al., 2003). Isomerization of the benzoquinone ansamycins has been proposed to be a key requirement for Hsp90 inhibition (Lee et al., 2004). An early co-crystallization study suggested that Hsp90 may bind to the benzoquinone ansamycins as they resemble mis-folded peptides (Stebbins et al., 1997).

Molecular Pharmacology Fast Forward. Published on February 1, 2011 as DOI: 10.1124/mol.110.070086
This article has not been copyedited and formatted. The final version may differ from this version.

Although the nucleotide-binding site of Hsp90 is not a recognized peptide-binding domain, the Hsp90-mediated isomerization of the benzoquinone ansamycins has been supported by quantum and molecular mechanic studies (Jez et al., 2003; Lee et al., 2004), and the *cis-trans* isomerization of non-proline peptide bonds (Schiene-Fischer et al., 2002). Other studies have proposed that a co-chaperone may have isomerase activity (Pearl and Prodromou, 2000; Kamal et al., 2003), and a recent study has disputed the isomerization of the benzoquinone ansamycins as a requirement for Hsp90 inhibition (Onuoha et al., 2007).

In addition to *trans-cis* isomerization, the C17 substituents of the benzoquinone ansamycins are extensively metabolized *in vivo* (Egorin et al., 1998), and the 19-position is prone to glutathionylation (Cysyk et al., 2006; Guo et al., 2008). The redox active quinone moiety is susceptible to one- and two-electron reduction by flavin-containing reductases (Guo et al., 2005; Lang et al., 2007). The direct two-electron reduction of benzoquinone ansamycins catalyzed by NAD(P)H:quinone oxidoreductase 1 (NQO1, DT-diaphorase, EC: 1.6.99.2) generating their hydroquinone derivatives circumvents the formation of semiquinone radicals and reactive oxygen species (Ross, 2004). Furthermore, NQO1 is expressed at high levels in many solid tumors (Siegel and Ross, 2000), and the expression of NQO1 has been found to correlate with 17AAG sensitivity (Kelland et al., 1999), offering the potential for drug activation with tumor selectivity (Rooseboom et al., 2004).

In our previous studies we reported the metabolism of a series of benzoquinone ansamycins by recombinant human (rh)NQO1 generating the corresponding hydroquinone ansamycins (Scheme 1), and these were more potent inhibitors of yeast Hsp90 ATPase activity than their parent quinones (Guo et al., 2005; Guo et al., 2006). This potentiated inhibition was rationalized by molecular modeling simulations that displayed increased direct hydrogen bond interactions between the hydroquinone ansamycins and the amino acid residues in the nucleotide-binding

site of Hsp90 (Guo et al., 2005; Guo et al., 2006). In this study, we extend our previous investigations using yeast Hsp90 to human Hsp90 (yeast Hsp90 has ~60% homology with human Hsp90). We have examined the relative rate of rhNQO1-mediated reduction of a series of benzoquinone ansamycins and the inhibition of purified human Hsp90 by both benzoquinone and hydroquinone ansamycins. Computational-based molecular docking was used to investigate the conformation of the benzoquinone ansamycins in the NQO1 active site and the structural properties that influence the rate of NQO1-mediated reduction. The interaction of the *trans*- and *cis*-amide isomers of the benzoquinone and hydroquinone ansamycins in the nucleotide-binding site of human Hsp90 was also investigated using molecular docking to explore the potential mechanism of Hsp90-mediated *trans-cis* isomerization.

Molecular Pharmacology Fast Forward. Published on February 1, 2011 as DOI: 10.1124/mol.110.070086
This article has not been copyedited and formatted. The final version may differ from this version.

Materials and Methods

Materials. GM, 17-demthoxy-17-[[2-(dimethylamino)ethyl]amino]-geldanamycin (17DMAG), and 17-demethoxy-17-[[2-(pyrrolidin-1-yl)ethyl]amino]-geldanamycin (17AEP-GA) were obtained from Invivogen Inc (San Diego, CA), and 17AAG and 17-(amino)-17-demethoxygeldanamycin (17AG) were obtained from the National Cancer Institute and Kosan Biosciences (Hayward, CA). 2,6-Dichlorophenol-indophenol (DCPIP), NADH, NADPH, bovine serum albumin (BSA), D(-)penicillamine were obtained from the Sigma Chemical Co. (St. Louis MO). Malachite green phosphate assay kit was obtained from BioAssay Systems Inc (Hayward CA). 5-Methoxy-1,2-dimethyl-3-[(4-nitrophenoxy)methyl]indole-4,7-dione (ES936) (Winski et al., 2001) was supplied by Professor Christopher J. Moody (School of Chemistry, University of Nottingham, Nottingham, United Kingdom). Human Hsp90 was a kind gift from Professor David Toft (Mayo Clinic College of Medicine, Rochester, MN). Recombinant human NQO1 was purified from *Escherichia coli* as described previously (Beall et al., 1994). The activity of rhNQO1 was 4.5 μmol DCPIP/min/mg.

HPLC and LC-MS Analysis. The NQO1-mediated reduction of the benzoquinone ansamycins was monitored by HPLC on a Luna C18 5 μm, 4.6 x 250mm reverse-phase column (Phenomenex, Torrance, CA) at room temperature. HPLC conditions were as follows: buffer A, 50 mM ammonium acetate (pH 4) containing 10 μM D(-)-penicillamine; buffer B, acetonitrile (100%). Both buffers were continuously bubbled with argon, gradient, 30% B to 90% B over 10 minutes and then 90% B for 5 minutes (flow rate of 1 mL/min). The sample injection volume was 50 μL. LC-MS was performed using positive ion electrospray ionization and mass spectra were obtained using a PE Sciex API-3000 triple quadrupole MS (Foster City, CA) with a turbo ion spray source interfaced to a PE Sciex 200 HPLC system. Samples were separated on a Luna C18 5 μm, 50 x 2 mm reverse-phase column (Phenomenex, Torrance, CA) using a gradient elution consisting of a 2 minute initial hold at 20% B followed by an increase to 80% B over 20

Molecular Pharmacology Fast Forward. Published on February 1, 2011 as DOI: 10.1124/mol.110.070086
This article has not been copyedited and formatted. The final version may differ from this version.

minutes at a flow rate of 200 µL/min and a sample injection volume of 20 µL. Solvent A, 10 mM ammonium acetate containing 0.1% (v/v) acetic acid (pH 4.4) and solvent B, 10 mM ammonium acetate in acetonitrile containing 0.1% (v/v) acetic acid. Mass spectra were continuously recorded from 150 to 1000 amu every 3 seconds during the chromatographic analysis, with a turbo ion spray temperature of 250ºC, spray needle voltage at 4,500V, declustering potential at 35V, and focus plate at 125V.

Reduction of Benzoquinone Ansamycins by rhNQO1. Benzoquinone ansamycin 50 µM, NADH 200 µM and rhNQO1 (1.65 µg for GM, 17AAG, and 17AG; 3.3 µg for 17DMAG; 6.6 µg for 17AEP-GA) in 50 mM potassium phosphate buffer, pH 7.4 (1 mL) containing 1 mg/mL BSA were incubated at 37ºC for 10 min. Reactions were monitored by HPLC and the reduction rate was determined by measuring NADH oxidation at 340nm during the reaction. The reaction was stopped with an equal volume of methanol. The apparent K_m values for 17AAG and 17DMAG (0.004–0.8 mmol/L) were determined using NADH 0.5 mmol/L, and rhNQO1 10 µg, incubated in 50 mM potassium phosphate buffer, pH 7.4 containing FAD (1 µmol/L), 0.4% (v/v) Tween-80 and 0.4% (v/v) TritonX-100 at 30°C and by monitoring quinone-dependant oxidation of NADH. Reactions were terminated by diluting the reaction 10X with ice-cold methanol and the resulting NADH concentrations were determined by fluorescence spectroscopy (ex 340nm, em 460nm). K_m values were determined using Prism software (GraphPad Software Inc, San Diego CA).

Hsp90 ATPase Activity Assay. Inhibition of human Hsp90 ATPase activity was measured as described previously (Rowlands et al., 2004; Guo et al., 2005). Briefly, 2.5 µg of purified human Hsp90 was incubated in 100 mM Tris-HCl (pH 7.4) containing KCl 20 mM, $MgCl_2$ 6 mM, NADH 200 µM, benzoqinone ansamycin (2 µM and 4 µM) with or without rhNQO1 0.33 µg, and with or without ES936 2 µM. Reactions (25 µL) were started by the addition of 1 mM ATP and allowed to proceed at 37ºC for 12 h. Reactions were then diluted with 225 µL of 100 mM Tris-HCl (pH

Molecular Pharmacology Fast Forward. Published on February 1, 2011 as DOI: 10.1124/mol.110.070086
This article has not been copyedited and formatted. The final version may differ from this version.

7.4) containing KCl 20 mM and $MgCl_2$ 6 mM mixed thoroughly, and 80 µL was transferred to a 96-well plate followed by 20 µL malachite green reagent. After 10 minutes, trisodium citrate (83 mM) was added to stabilize the color and plates were read at 650 nm.

Molecular Modeling. All simulations were performed using Discovery Studio software (Version 2.5; Accelrys Inc., San Diego, CA). The crystallographic coordinates of the 1.8Å human NQO1 structure co-crystallized with ES936, (PDB: 1KBQ) , the 2.2Å open human Hsp90 structure, (PDB: 1YES) and the 1.9Å human Hsp90 structure co-crystallized with GM (PDB: 1YET) (Stebbins et al., 1997; Winski et al., 2001), were obtained from the RCSB Protein Data Bank (http://www.rcsb.org). The *cis*-amide isomers of the benzoquinone ansamycins were constructed from GM isolated from the human Hsp90-GM co-crystallized complex, the *trans*-amide isomers were constructed from *trans*-17-azetidinyl-17-demethoxygeldanamycin (Schnur and Corman, 1994), obtained from the Cambridge Structural Database (http://www.ccdc.cam.ac.uk), and the corresponding hydroquinone ansamycins were generated by modifying the quinone ring structure. The ionizable residues were corrected for physiologic pH, and the potentials and charges of the complexes were corrected using CHARMm in all simulations (Brooks et al., 2009).

NQO1 Docking. The ES936 molecules were removed from the NQO1 structure and the anionic form of reduced FAD was constructed from each FAD co-factor (Reigan et al., 2007). The binding site was defined as whole residues within a 5Å radius subset encompassing the FAD co-factor. The flexible docking program was used to dock the *trans*-amide isomers of the benzoquinone ansamycins into the NQO1 active site, followed by simulated annealing step to optimize interactions (Koska et al., 2008). In addition to the benzoquinone ansamycin, flexibility was allowed in the following active site R-groups: Leu103, Gln104, Trp105, Phe106, Thr148, Gly149, Gly150, Ser151, Met154, Tyr155, His161, Pro68, Gly122, Tyr126, Thr127, Tyr128,

Molecular Pharmacology Fast Forward. Published on February 1, 2011 as DOI: 10.1124/mol.110.070086
This article has not been copyedited and formatted. The final version may differ from this version.

Met131, Phe178, Phe232, and the FAD co-factor. An *in situ* minimization using the conjugate gradient method (1000 iterations with an RMS cut-off of 0.001kcal/mol) coupled with the Poisson-Boltzman surface area implicit solvent model, was used to calculate binding energy for each docked pose (Feig et al., 2004).

Hsp90 Docking. The *cis*- and *trans*-isomers of the benzoquinone and hydroquinone ansamycins were docked separately into the nucleotide-binding site of the open human Hsp90 structure, defined as whole residues within a 4Å radius subset. The flexible docking program was used to dock the benzoquinone and hydroquinone ansamycins into the nucleotide-binding site of Hsp90, which was followed by a minimization using the conjugate gradient method (1000 iterations with an RMS cut-off of 0.001kcal/mol). Flexibility was allowed in the following active site R-groups: Ile26, Glu47, Leu48, Ser50, Asn51, Ser52, Asp54, Ala55, Lys58, Ile96, Gly97, Met98, Asp102, Leu103, Asn105, Asn106, Leu107, Gly108, Ile110, Lys112, Gly132, Gly135, Val136, Gly137, Phe138, Tyr139, Val150, and Thr184.The interaction of the *cis*-amide isomers of the benzoquinone and hydroquinone ansamycins with Hsp90 were further examined using the human Hsp90 structure co-crystallized with GM. The co-crystallized GM structure was removed and the *cis*-amide isomers of the benzoquinone and hydroquinone ansamycins were in turn docked into the nucleotide-binding domain of Hsp90 using the same docking method for the open Hsp90 structure. The Poisson Boltzman implicit solvent model used in NQO1 docking was used to calculate the binding energy for each docked pose.

Molecular Pharmacology Fast Forward. Published on February 1, 2011 as DOI: 10.1124/mol.110.070086
This article has not been copyedited and formatted. The final version may differ from this version.

Results

NQO1-mediated Reduction of Benzoquinone Ansamycins. The benzoquinone ansamycins, GM, 17AAG, 17AG, 17DMAG, and 17AEP-GA, were all reduced by purified rhNQO1, using either NADH or NADPH as cofactors, to the corresponding hydroquinone ansamycins without further metabolism. The reduction of the benzoquinone ansamycins by rhNQO1 was monitored spectrophotometrically and the generation of the polar hydroquinone ansamycin was proportional to the loss of benzoquinone ansamycin (see supplemental data). The hydroquinone ansamycins were identified by LC-MS and mass ions were observed for $17AAGH_2$ at *m/z* 603.7 $[M+NH_4]^+$, GMH_2 at *m/z* 580.5 $[M+NH_4]^+$, $17AGH_2$ at *m/z* 548.2 $[M+H]^+$, $17DMAGH_2$ at *m/z* 619.3 $[M+H]^+$, and 17AEP-GAH_2 at *m/z* 645.3 $[M+H]^+$ (see supplemental data). The relative rhNQO1-mediated reduction rate for this series of benzoquinone ansamycins was dependent on the C17 substituent and fastest for 17AAG, followed by 17AG, GM, 17DMAG, and then 17AEP-GA (Figure 1). The NQO1-dependent formation of the hydroquinone ansamycin from the parent quinone was prevented by ES936, a mechanism-based inhibitor of NQO1 (see supplemental data). Apparent K_m values were determined for the NQO1-mediated reduction of 17AAG (189 μM) and 17DMAG (262 μM) (see supplemental data).

Molecular Docking of the *trans*-Amide Isomers of the Benzoquinone Ansamycins into Human NQO1. Molecular docking simulations demonstrated that the *trans*-amide isomers of this benzoquinone ansamycin series could be accommodated within the active site of NQO1. The reduced anionic form of the FAD cofactor was used in these docking studies as this represents the NQO1 enzyme at the beginning of the catalytic cycle, when the enzyme can accept the quinone substrate prior to reduction to the hydroquinone (Li et al., 1995; Cavelier and Amzel, 2001). The flexible docking program generated 50 structural complexes for 17AAG, 41 for 17AG, 21 for GM, 15 for 17DMAG, and 11 for 17AEP-GA. The resultant complexes were

Molecular Pharmacology Fast Forward. Published on February 1, 2011 as DOI: 10.1124/mol.110.070086
This article has not been copyedited and formatted. The final version may differ from this version.

evaluated based on the calculated binding energy, the number of hydrogen bond interactions between NQO1 and the benzoquinone ansamycin, and the position of the quinone ring in the active site of NQO1. A reoccurring high-ranking binding conformation was identified for each benzoquinone ansamycin in this series, where the quinone moiety was parallel to the isoalloxazine ring of the flavin cofactor, optimizing π-π interactions and increasing the van der Waals contribution to the binding energy. In this conformation the C21 carbonyl of the benzoquinone ansamycin displayed a hydrogen bond with Tyr128, the C17 substituent occupied the cleft formed by Tyr155, His161, His194, Phe232, and Phe236, and the majority of the ansa ring was outside of the active site (Figure 2). In this series of benzoquinone ansamycins 17AAG had the most favorable binding energy followed by 17AG, GM, 17DMAG, and then 17AEP-GA, for this conformation (Table 1). In addition, the binding energies obtained for the highest ranked pose for each benzoquinone ansamycin correlates with the distance between the C21 carbonyl of the quinione and Tyr128, which would suggest that the benzoquinone ansamycins with small C17 substituents are accommodated by NQO1 more readily that benzoquinone ansamycins with large C17 substituents. The docking of the *cis*-amide isomers of the benzoquinone ansmaycins was attempted, but this was unsuccessful due to steric conflicts with active site residues.

Inhibition of Human Hsp90 ATPase Activity. The inhibition of human Hsp90 ATPase activity by this series of benzoquinone and hydroquinone ansamycins was evaluated using the malachite green phosphate assay (Rowlands et al., 2004). The inhibition of human Hsp90 ATPase activity was assessed with only 17AAG and 17AAGH_2 (Guo et al., 2005). The benzoquinone ansamycins did inhibit the ATPase activity of human Hsp90 at the concentrations investigated; however, inhibition significantly increased when the benzoquinone ansamycins were incubated with rhNQO1, and this increased inhibition was abrogated by pre-treatment with ES936 (Figure 3). These results clearly demonstrate that the hydroquinone ansamycins

Molecular Pharmacology Fast Forward. Published on February 1, 2011 as DOI: 10.1124/mol.110.070086
This article has not been copyedited and formatted. The final version may differ from this version.

generated by NQO1 were more potent inhibitors of Hsp90 ATPase activity than the corresponding benzoquinone ansamycins, in agreement with our previous data using yeast Hsp90 (Guo et al., 2005; Guo et al., 2006).

Molecular Docking of the *trans*- and *cis*-Amide Isomers of the Benzoquinone and Hydroquinone Ansamycins into Human Hsp90. Previous studies had reported that it was not possible to dock the *trans*-amide isomers of the benzoquinone ansamycins into the Hsp90 structure; however, these studies used the human Hsp90 structure co-crystallized with GM or 17DMAG (Jez et al., 2003; Lee et al., 2004). In this study the *trans*- and *cis*-amide isomers of the benzoquinone and hydroquinone ansamycins were successfully docked into the nucleotide-binding domain of the open Hsp90 structure (Stebbins et al., 1997). The calculated binding energies values indicate greater stability between the hydroquinone ansamycin and Hsp90 than the parent quinone. Similar high scoring conformations were observed across the benzoquinone and hydroquinone ansamycin series for the *trans*- and *cis*-amide isomers, all with favorable dock scores and binding energies for binding to the Hsp90 protein (Table 2 data shown for 17AAG; for other compounds, see supplemental data). The overall conformation of the quinone or hydroquinone and the ansa ring were similar for the *trans*-amide isomers of the benzoquinone and hydroquinone ansamycins in the nucleotide-binding domain of the open human Hsp90 structure (Figure 4A and B representations shown for 17AAG; for other compounds, see supplemental data). However, differences were observed in the orientation of the C17 substituent outside of the binding pocket, with the exception of 17AG and $17AGH_2$, the C17 substituents of the benzoquinone ansamycins were almost perpendicular to the plane of the quinone, and in the case of the hydroquinone ansamycins they extended in the plane of the hydroquinone. There were few hydrogen bond interactions between the *trans*-amide isomers and the Hsp90 protein, the most notable being the interactions between the C18 carbonyl of 17AAG and 17AG with Ser113 and the C18 hydroxyl of $17AGH_2$ and $17AEP\text{-}GAH_2$ with Gly135.

Molecular Pharmacology Fast Forward. Published on February 1, 2011 as DOI: 10.1124/mol.110.070086
This article has not been copyedited and formatted. The final version may differ from this version.

Interestingly, although no hydrogen bond interactions were observed between Lys112 and the hydroquinone ansamycins, with the exception of 17AEP- GAH_2, the NH_3^+ group of Lys112 was directed towards the hydroquinone ring. This was in contrast to the benzoquinone ansamycins, where the NH_3^+ group of Lys112 was directed away from the quinone ring.

The conformations of the *cis*-amide isomers of the benzoquinone and hydroquinone ansamycins were similar in the nucleotide-binding site of the open Hsp90 structure, and with the exception of GM and GMH_2, the C17 substituents of the benzoquinone and hydroquinone ansamycins adopted a similar arrangement outside of the binding pocket. A greater number of hydrogen bond interactions were observed between the hydroquinone ansamycins with a C17 amino substituent and the open Hsp90 structure compared with the corresponding benzoquinone ansamycins (Figure 4C and D representations shown for 17AAG; for other compounds, see supplemental data). The hydroquinone ansamycins displayed additional hydrogen bond interactions between the C18 hydroxyl and Asp54, and this hydrogen bond was observed with GMH_2; however, no hydrogen bond interactions were observed between the C17 substituent of GM or GMH_2 and the open Hsp90 structure. GM was the only benzoquinone ansamycin to display an additional hydrogen bond between the C1 amino and Gly135, resulting in GM and GMH_2 having an equal number of hydrogen bond interactions with the open Hsp90 structure. The docking of the *trans*- and *cis*-amide hydroquinone ansamycins in this series into the open Hsp90 structure resulted in more favorable dock scores and calculated binding energy values, than the corresponding benzoquinone ansamycins, and this was largely due to the increased contribution of electrostatic energy (Table 2 data shown for 17AAG; for other compounds, see supplemental data).

The docking of the benzoquinone and hydroquinone ansamycins into the GM bound form of human Hsp90 (Stebbins et al., 1997), resulted in similar conformations and interactions to those

Molecular Pharmacology Fast Forward. Published on February 1, 2011 as DOI: 10.1124/mol.110.070086
This article has not been copyedited and formatted. The final version may differ from this version.

reported in the co-crystallized structures (Stebbins et al., 1997; Jez et al., 2003). In these studies only the *cis*-amide isomers of the benzoquinone and hydroquinone ansamycins were used, as the *trans*-amide isomers could not be positioned into the nucleotide-binding domain without steric conflicts with active site residues. Consistent with previous studies, using the yeast Hsp90 crystal structure (Guo et al., 2005; Guo et al., 2006), the hydroquinone ansamycins displayed additional hydrogen bond interactions with the human Hsp90 protein compared with the parent quinone (Figure 4E and F representations shown for 17AAG; for other compounds, see supplemental data). The C18 hydroxyl interacts with the carboxylate side chain of Asp40 and allows for further interaction between the C17 substituent and the Asp54 and Lys58. These additional hydrogen bond interactions between the hydroquinone ansamycin and the Hsp90 protein result in a more compact C-clamp conformation around Helix-2, and these additional interactions translate into more favorable calculated binding energies than those of the parent quinones (Table 3 data shown for 17AAG; for other compounds, see supplemental data), providing a structural explanation as to why the hydroquinone ansamycins are more potent Hsp90 inhibitors.

Molecular Pharmacology Fast Forward. Published on February 1, 2011 as DOI: 10.1124/mol.110.070086
This article has not been copyedited and formatted. The final version may differ from this version.

Discussion

The amide bond in the ansa ring of the benzoquinone and hydroquinone ansamycins restricts rotation and consequently only *trans*- and *cis*-amide conformations are possible. The benzoquinone ansamycins adopt the *trans*-amide conformation in solution, as this is energetically favored (Schnur and Corman, 1994; Jez et al., 2003), and co-crystallization studies have clearly shown the *cis*-amide isomer is bound to Hsp90 (Stebbins et al., 1997; Jez et al., 2003), indicating that *trans*-*cis* isomerization of the benzoquinone ansamycins must occur during the binding process. However, a recent study concluded that no isomerization step occurs in the binding of the benzoquinone ansamycins to Hsp90 (Onuoha et al., 2007), and proposed that small quantities of the *cis*-amide isomer in solution, identified in an NMR study (Thepchatri et al., 2007), may bind directly to Hsp90 and *in vivo* potency could be due to the direct binding of the hydroquinone of the *cis*-amide isomer. This counters the results of a study examining the effects of conformationally constrained *cis*-amide chimeric inhibitors of Hsp90 (Duerfeldt et al., 2009), and our molecular docking studies where the *cis*-amide isomer would not dock into NQO1. However, the results of a binding affinity study using BODIPY-geldanamycin in the absence and presence of reducing agents reported by Onuoha *et al* may in fact support Hsp90-mediated isomerization. The binding affinity was time-dependent in the absence of reducing agents indicating that the benzoquinone ansamycins weakly bind Hsp90 initially and then undergo a structural change, in agreement with a prior study (Gooljarsingh et al., 2006). The non-time-dependent increased binding affinity in the presence of reducing agents may be due to the formation of the hydroquinone and the *cis*-amide isomer, as reducing agents were used to catalyze tautomerization (Clarke et al., 1984; Schmid, 1993). The Hsp90-mediated isomerization of the benzoquinone ansamycins has also been supported by quantum and molecular mechanic studies (Jez et al., 2003; Lee et al., 2004), and the identification of non-prolyl peptide *cis*-*trans* isomerases (Bouckaert et al., 2000; Schiene-Fischer et al., 2002).

Molecular Pharmacology Fast Forward. Published on February 1, 2011 as DOI: 10.1124/mol.110.070086
This article has not been copyedited and formatted. The final version may differ from this version.

Lee *et al*, proposed that Lys112 and Ser113 of Hsp90 interact with the C1 amide of the benzoquinone ansamycin promoting isomerization *via* tautomerization, and based on the loss of GM binding to a Ser113 Hsp90 point mutant they determined that Ser113 was essential for Hsp90-mediated *trans-cis* isomerization (Lee et al., 2004). However, the mutation of Ser113 may in turn affect the conformation of Lys112 in the nucleotide-binding site. Although the initial benzoquinone ansamycin binding pose described by Lee *et al* was not identified in our docking studies and no interactions were observed between the C1 amide of the benzoquinone or hydroquinone ansamycins and Lys112 or Ser113 residues of Hsp90, the results of our docking studies provide support for the model of Hsp90-mediated *trans-cis* isomerization through promoting tautomerization and suggest Lys112 is an important mediator in this process.

The benzoquinone ansamycin series examined in our study were metabolized by rhNQO1 to generate the corresponding hydroquinone ansamycins and these were more potent inhibitors of purified human Hsp90 than their parent quinones. The potentiated inhibition of Hsp90 by the hydroquinone ansamycins was rationalized by the increased hydrogen bond interactions between the hydroquinone ansamycins and the Hsp90 protein using computational-based modeling. The interaction of the *trans*- and *cis*-amide isomers of the benzoquinone and hydroquinone ansamycins in the open human Hsp90 structure provide support for Hsp90-mediated isomerization. In all cases the hydroquinone ansamycins had more favorable binding energies than the parent quinones, indicating that both the *trans*- and *cis*-amide isomers of the hydroquinone ansamycins would exhibit increased binding affinity for Hsp90. Modeling studies support that the *trans*-amide isomer of the benzoquinone and hydroquinone ansamycins bind to Hsp90 and this would be a critical initial step for Hsp90-mediated isomerization. This could also rationalize the results of mutational studies (Lee et al., 2004), as mutating the Lys112 and/or the Ser113 residues could impede Hsp90-mediated isomerization but it would not obstruct the binding of the *trans*-amide isomer. The high-scoring complexes of the *trans*-amide isomers in

Molecular Pharmacology Fast Forward. Published on February 1, 2011 as DOI: 10.1124/mol.110.070086
This article has not been copyedited and formatted. The final version may differ from this version.

the open human Hsp90 structure, identified in our study, may represent the initial binding conformation of the benzoquinone and hydroquinone ansamycins. The C18 carbonyl of the *trans*-amide isomer of 17AAG and 17AG displayed a hydrogen bond interaction with Ser113. The deprotonation of the amide nitrogen of the benzoquinone ansmycins may allow the C1 amide or the C18 carbonyl to abstract a proton from Ser113, promoting tautomerization of the amide via a proton shuttle between the quinone and the amide (Scheme 2A). In response to the change in the electronic properties of the quinone ring, Lys112 may then move to protonate the nitrogen of the imine. The destabilization of the hydroquinone ring is not required for the isomerization of the hydroquinone ansamycins (Scheme 2B), since Lys112 is in close proximity to the nitrogen of the C1 amide, to donate a proton, if required (Figure 5). The interaction between the Lys112 residue and the lone pair of electrons of the amide nitrogen acts to deconjugate the resonance of the amide bond and promote *trans*-*cis* isomerization.

This proposed acid catalyzed *trans*-*cis* isomerization mechanism is similar to that described for the peptidyl-prolyl isomerases (PPIases). Although the precise mechanism of peptidyl-prolyl *cis*-*trans* isomerization catalyzed by PPIases remains to be fully elucidated, it is widely accepted that the protonation of the imine nitrogen is the fundamental step in enzyme-catalyzed isomerization (Schmid, 1993; Hur and Bruice, 2002). *Cis*-*trans* isomerization of prolyl peptides by the cyclophilin PPIases involves the stabilization of the amide oxygen by an Asn residue, the proline ring is held in position by the phenyl group of a Phe residue, and the guanidino group of a conserved Arg residue weakens the double bond character of the C-N bond (Hur and Bruice, 2002). Similar interactions were observed between the *trans*-amide isomers of the benzoquinone and hydroquinone ansamycins and the open Hsp90 structure, with Ser113 and Phe138 stabilizing benzoquinone and hydroquinone ansamycin binding, and the NH_3^+ group of Lys112 is available to protonate the imine nitrogen promoting the keto tautomer. The intrinsic structural properties of the ansamycin ring, the anchoring of the carbamate through interaction

with Asp90 at the base of the nucleotide-binding domain, and the interaction of the ansa ring with amino acid residues *via* through-bond interactions with the specific solvent network in the nucleotide-binding domain, may also aid to drive *trans-cis* isomerization (Pappenberger et al., 2001). The confirmation of Hsp90-mediated *trans-cis* isomerization of the benzoquinone and hydroquinone ansamycins is important since it could be exploited in the development of new Hsp90 inhibitors, and recently the effect of conformationally restrained *cis*-amide isomers of benzoquinone ansamycin analogs on Hsp90 inhibition has been reported (Duerfeldt et al., 2009).

The rate of NQO1-mediated reduction of this benzoquinone ansamycin series was dependent on the C17 substituent, and fastest for 17AAG due to the small size of the C17 substituent and the additional interactions between the allyl group and active site residues. The allyl substituent of 17AAG is almost perpendicular to the plane of the phenoxy of Tyr155 further increasing the van der Waals contribution to the calculated binding energy through π-π interactions. The C17 amino and methoxy substituents of 17AG and GM are small enough to be accommodated by the NQO1 active site; however, the large 2-(dimethylamino)ethyl and 2-(pyrrolidinyl-1-yl)ethyl substituents of 17DMAG and 17AEP-GA are directed away from His161 and Tyr155 and their steric bulk would restrict the quinone from entering the active site, and this is reflected in the relative reduction rate. The difference between the relative rates of NQO1-mediated reduction of 17AAG and 17DMAG was approximately 3-fold. Interestingly, the ranking order of the calculated binding energy associated with the benzoquinone ansamycin binding conformation was also in agreement with the order of the relative reduction rate using purified rhNQO1.

The selective generation of the hydroquinone ansamycins within the cancer cell is desirable as this will result in potentiated Hsp90 inhibition, and increased cell retention and accumulation, compared with the parent quinone. The properties of the C17 substituent and the metabolism of

Molecular Pharmacology Fast Forward. Published on February 1, 2011 as DOI: 10.1124/mol.110.070086
This article has not been copyedited and formatted. The final version may differ from this version.

the benzoquinone ansamycin, by NQO1 and other oxidoreductases, should be considered in the development of further benzoquinone ansamycins. The rational progression of this approach would be to develop a stable, water-soluble prodrug that protects the hydroquinone group, and is activated via intracellular enzymatic hydrolysis generating a relatively stable hydroquinone ansamycin and potent Hsp90 inhibitor, which in its quinone form would be an efficient substrate for NQO1.

Molecular Pharmacology Fast Forward. Published on February 1, 2011 as DOI: 10.1124/mol.110.070086
This article has not been copyedited and formatted. The final version may differ from this version.

Acknowledgements

We acknowledge Dr. Daniel L. Gustafson and Joeseph Zirolli for their assistance with mass spectral determinations. The authors disclose a pending patent interest in hydroquinone ansamycins and their prodrugs (International Application No: PCT/US2005/031524).

Authorship Contribution
Participated in research design: Reigan, Siegel, Ross
Conducted experiments: Reigan, Siegel, Guo
Performed data analysis: Reigan, Seigel, Guo
Wrote or contributed to the writing of the manuscript: Reigan, Ross

References

Beall HD, Mulcahy RT, Siegel D, Traver RD, Gibson NW and Ross D (1994) Metabolism of bioreductive antitumor compounds by purified rat and human DT-diaphorases. *Cancer Res* **54:**3196-3201.

Bouckaert J, Dewallef Y, Poortmans F, Wyns L and Loris R (2000) The structural features of concanavalin A governing non-proline peptide isomerization. *J Biol Chem* **275:**19778-19787.

Brooks BR, Brooks CL, 3rd, Mackerell AD, Jr., Nilsson L, Petrella RJ, Roux B, Won Y, Archontis G, Bartels C, Boresch S, Caflisch A, Caves L, Cui Q, Dinner AR, Feig M, Fischer S, Gao J, Hodoscek M, Im W, Kuczera K, Lazaridis T, Ma J, Ovchinnikov V, Paci E, Pastor RW, Post CB, Pu JZ, Schaefer M, Tidor B, Venable RM, Woodcock HL, Wu X, Yang W, York DM and Karplus M (2009) CHARMM: the biomolecular simulation program. *J Comput Chem* **30:**1545-1614.

Cavelier G and Amzel LM (2001) Mechanism of NAD(P)H:quinone reductase: *Ab initio* studies of reduced flavin. *Proteins* **43:**420-432.

Chiosis G, Huezo H, Rosen N, Mimnaugh E, Whitesell L and Neckers L (2003) 17AAG: low target binding affinity and potent cell activity--finding an explanation. *Mol Cancer Ther* **2:**123-129.

Chiosis G and Neckers L (2006) Tumor selectivity of Hsp90 inhibitors: the explanation remains elusive. *ACS Chem Biol* **1:**279-284.

Clarke ED, Wardman P and Wilson I (1984) *Cis-trans* isomerization of the (5-nitro-2-furyl)acrylamide, AF-2, initiated by ascorbate, glutathione, Fe(II) and OH. *Biochem Pharmacol* **33:**83-87.

Cysyk RL, Parker RJ, Barchi JJ, Jr., Steeg PS, Hartman NR and Strong JM (2006) Reaction of geldanamycin and C17-substituted analogues with glutathione: product identifications and pharmacological implications. *Chem Res Toxicol* **19:**376-381.

Duerfeldt AS, Brandt GE and Blagg BS (2009) Design, synthesis, and biological evaluation of conformationally constrained *cis*-amide Hsp90 inhibitors. *Org Lett* **11:**2353-2356.

Egorin MJ, Rosen DM, Wolff JH, Callery PS, Musser SM and Eiseman JL (1998) Metabolism of 17-(allylamino)-17-demethoxygeldanamycin (NSC 330507) by murine and human hepatic preparations. *Cancer Res* **58:**2385-2396.

Feig M, Onufriev A, Lee MS, Im W, Case DA and Brooks CL, 3rd (2004) Performance comparison of generalized born and Poisson methods in the calculation of electrostatic solvation energies for protein structures. *J Comput Chem* **25:**265-284.

Gooljarsingh LT, Fernandes C, Yan K, Zhang H, Grooms M, Johanson K, Sinnamon RH, Kirkpatrick RB, Kerrigan J, Lewis T, Arnone M, King AJ, Lai Z, Copeland RA and Tummino PJ (2006) A biochemical rationale for the anticancer effects of Hsp90 inhibitors: slow, tight binding inhibition by geldanamycin and its analogues. *Proc Natl Acad Sci U S A* **103:**7625-7630.

Guo W, Reigan P, Siegel D and Ross D (2008) Enzymatic reduction and glutathione conjugation of benzoquinone ansamycin Hsp90 inhibitors: Relevance for toxicity and mechanism of action. *Drug Metab Dispos* **36:**2050-2057.

Guo W, Reigan P, Siegel D, Zirrolli J, Gustafson D and Ross D (2005) Formation of 17-allylamino-demethoxygeldanamycin (17-AAG) hydroquinone by NAD(P)H:quinone oxidoreductase 1: role of 17-AAG hydroquinone in heat shock protein 90 inhibition. *Cancer Res* **65:**10006-10015.

Guo W, Reigan P, Siegel D, Zirrolli J, Gustafson D and Ross D (2006) The bioreduction of a series of benzoquinone ansamycins by NAD(P)H:quinone oxidoreductase 1 to more potent heat shock protein 90 inhibitors, the hydroquinone ansamycins. *Mol Pharmacol* **70:**1194-1203.

Hur S and Bruice TC (2002) The mechanism of *cis-trans* isomerization of prolyl peptides by cyclophilin. *J Am Chem Soc* **124:**7303-7313.

Jez JM, Chen JC, Rastelli G, Stroud RM and Santi DV (2003) Crystal structure and molecular modeling of 17-DMAG in complex with human Hsp90. *Chem Biol* **10:**361-368.

Kamal A, Thao L, Sensintaffar J, Zhang L, Boehm MF, Fritz LC and Burrows FJ (2003) A high-affinity conformation of Hsp90 confers tumour selectivity on Hsp90 inhibitors. *Nature* **425:**407-410.

Kelland LR, Sharp SY, Rogers PM, Myers TG and Workman P (1999) DT-Diaphorase expression and tumor cell sensitivity to 17-allylamino, 17-demethoxygeldanamycin, an inhibitor of heat shock protein 90. *J Natl Cancer Inst* **91:**1940-1949.

Koska J, Spassov VZ, Maynard AJ, Yan L, Austin N, Flook PK and Venkatachalam CM (2008) Fully automated molecular mechanics based induced fit protein-ligand docking method. *J Chem Inf Model* **48:**1965-1973.

Lang W, Caldwell GW, Li J, Leo GC, Jones WJ and Masucci JA (2007) Biotransformation of geldanamycin and 17-allylamino-17-demethoxygeldanamycin by human liver microsomes: reductive versus oxidative metabolism and implications. *Drug Metab Dispos* **35:**21-29.

Lee YS, Marcu MG and Neckers L (2004) Quantum chemical calculations and mutational analysis suggest heat shock protein 90 catalyzes *trans-cis* isomerization of geldanamycin. *Chem Biol* **11:**991-998.

Li R, Bianchet MA, Talalay P and Amzel LM (1995) The three-dimensional structure of NAD(P)H:quinone reductase, a flavoprotein involved in cancer chemoprotection and chemotherapy: mechanism of the two-electron reduction. *Proc Natl Acad Sci U S A* **92:**8846-8850.

Maloney A and Workman P (2002) HSP90 as a new therapeutic target for cancer therapy: the story unfolds. *Expert Opin Biol Ther* **2:**3-24.

Onuoha SC, Mukund SR, Coulstock ET, Sengerova B, Shaw J, McLaughlin SH and Jackson SE (2007) Mechanistic studies on Hsp90 inhibition by ansamycin derivatives. *J Mol Biol* **372:**287-297.

Pappenberger G, Aygun H, Engels JW, Reimer U, Fischer G and Kiefhaber T (2001) Nonprolyl *cis* peptide bonds in unfolded proteins cause complex folding kinetics. *Nat Struct Biol* **8:**452-458.

Pearl LH and Prodromou C (2000) Structure and *in vivo* function of Hsp90. *Curr Opin Struct Biol* **10:**46-51.

Pearl LH and Prodromou C (2006) Structure and mechanism of the Hsp90 molecular chaperone machinery. *Annu Rev Biochem* **75:**271-294.

Reigan P, Colucci MA, Siegel D, Chilloux A, Moody CJ and Ross D (2007) Development of indolequinone mechanism-based inhibitors of NAD(P)H:quinone oxidoreductase 1 (NQO1): NQO1 inhibition and growth inhibitory activity in human pancreatic MIA PaCa-2 cancer cells. *Biochemistry* **46:**5941-5950.

Roe SM, Prodromou C, O'Brien R, Ladbury JE, Piper PW and Pearl LH (1999) Structural basis for inhibition of the Hsp90 molecular chaperone by the antitumor antibiotics radicicol and geldanamycin. *J Med Chem* **42:**260-266.

Rooseboom M, Commandeur JN and Vermeulen NP (2004) Enzyme-catalyzed activation of anticancer prodrugs. *Pharmacol Rev* **56:**53-102.

Ross D (2004) Quinone reductases multitasking in the metabolic world. *Drug Metab Rev* **36:**639-654.

Rowlands MG, Newbatt YM, Prodromou C, Pearl LH, Workman P and Aherne W (2004) High-throughput screening assay for inhibitors of heat-shock protein 90 ATPase activity. *Anal Biochem* **327:**176-183.

Schiene-Fischer C, Habazettl J, Schmid FX and Fischer G (2002) The hsp70 chaperone DnaK is a secondary amide peptide bond cis-trans isomerase. *Nat Struct Biol* **9:**419-424.

Schmid FX (1993) Prolyl isomerase: enzymatic catalysis of slow protein-folding reactions. *Annu Rev Biophys Biomol Struct* **22:**123-142.

Schnur R and Corman ML (1994) Tandem [3,3]-sigmatropic rearrangements in an ansamycin-stereospecific conversion of an (S)-allylic alcohol to an (S)-allylic amine derivative. *J Org Chem* **59:**2581–2584.

Siegel D and Ross D (2000) Immunodetection of NAD(P)H:quinone oxidoreductase 1 (NQO1) in human tissues. *Free Radic Biol Med* **29:**246-253.

Stebbins CE, Russo AA, Schneider C, Rosen N, Hartl FU and Pavletich NP (1997) Crystal structure of an Hsp90-geldanamycin complex: targeting of a protein chaperone by an antitumor agent. *Cell* **89:**239-250.

Thepchatri P, Eliseo T, Cicero DO, Myles D and Snyder JP (2007) Relationship among ligand conformations in solution, in the solid state, and at the Hsp90 binding site: geldanamycin and radicicol. *J Am Chem Soc* **129:**3127-3134.

Winski SL, Faig M, Bianchet MA, Siegel D, Swann E, Fung K, Duncan MW, Moody CJ, Amzel LM and Ross D (2001) Characterization of a mechanism-based inhibitor of NAD(P)H:quinone oxidoreductase 1 by biochemical, X-ray crystallographic, and mass spectrometric approaches. *Biochemistry* **40:**15135-15142.

Molecular Pharmacology Fast Forward. Published on February 1, 2011 as DOI: 10.1124/mol.110.070086
This article has not been copyedited and formatted. The final version may differ from this version.

Footnotes

This work was supported by National Institute of Health grant R01-CA51210.

Molecular Pharmacology Fast Forward. Published on February 1, 2011 as DOI: 10.1124/mol.110.070086
This article has not been copyedited and formatted. The final version may differ from this version.

Scheme and Figure Legends

Scheme 1. The NQO1-mediated reduction of the benzoquinone ansamycins.

Scheme 2. The proposed mechanism of *trans-cis* isomerization of the A) benzoquinone ansamycins and the B) hydroquinone ansamycins. Arrows with broken lines indicate bond rotation.

Figure 1. Relative NQO1-mediated reduction rate of the benzoquinone ansamycins. Columns, mean (n = 3); bars, SD. GM, 17AG, 17DMAG and 17AEP-GA was significantly different from 17AAG, *p<0.01, **p<0.001. Statistical analysis was performed using one-way ANOVA with Tukey multiple comparison test.

Figure 2. Flat ribbon representation of human NQO1 in complex with the *trans*-amide isomer of A) 17AAG, B) GM, C) 17AG, D) 17DMAG, E) 17AEP-GA (stick display style; colored by atom type, carbon atoms colored yellow) in the reduced anionic FAD (stick display style; colored by atom type, carbon atoms colored orange) site, key amino acid residues (stick display style; colored by atom type), and hydrogen bond interactions (black dashed lines) are displayed.

Figure 3. Inhibition of human Hsp90 ATPase activity by 17AAG and $17AAGH_2$. Human Hsp90 ATPase activity was measured in reactions with either vehicle (DMSO) or A) 17AAG, B) GM, C) 17AG, D) 17DMAG, or E) 17AEP-GA (2μM and 4μM) in the presence and absence of rhNQO1. The reactions were analyzed after 12 h, and phosphate concentrations were measured using the malachite green assay. Open columns, benzoquinone ansamycin and NADH; filled columns, benzoquinone ansamycin, NADH, and rhNQO1; hatched columns, benzoquinone ansamycin, NADH, NQO1, and ES936. Columns, mean (n=3); bars, SD. Hsp90 ATPase activity in

Molecular Pharmacology Fast Forward. Published on February 1, 2011 as DOI: 10.1124/mol.110.070086
This article has not been copyedited and formatted. The final version may differ from this version.

incubates containing benzoquinone ansamycin, NADH, and NQO1 were statistically different from incubates containing benzoquinone ansamycin and NADH or benzoquinone ansamycin, NADH, NQO1, and ES936, *p<0.05, one-way ANOVA with Tukey for pairwise comparison. Data for 17AAG has been previously presented;[28] the experiment was repeated and the data is shown here to complete the comparison of all compounds in this structural series.

Figure 4. The human Hsp90-17AAG/17AAGH$_2$ complex. The nucleotide-binding domain of open human Hsp90 in complex with the *trans*-amide isomer of A) 17AAG and B) 17AAGH$_2$ and the *cis*-amide isomer of C) 17AAG and D) 17AAGH$_2$. The nucleotide-binding domain of bound human Hsp90 in complex with the *cis*-amide isomer of E) 17AAG and F) 17AAGH$_2$. 17AAG and 17AAGH$_2$ (stick display style; carbon atoms colored yellow) in the nucleotide-binding domain of Hsp90, key amino acid residues (stick display style; colored by atom type), and hydrogen bond interactions (black dashed lines) are displayed.

Figure 5. The interaction of A) *trans*-17AAG and B) *trans*-17AAGH$_2$ with Lys112 in the nucleotide-binding domain of human Hsp90.

Molecular Pharmacology Fast Forward. Published on February 1, 2011 as DOI: 10.1124/mol.110.070086
This article has not been copyedited and formatted. The final version may differ from this version.

Tables

Compound	ΔV_{vdw} (kcal/mol)	ΔV_{elect} (kcal/mol)	ΔG_{bind} (kcal/mol)	H-Bond Interaction		H-Bond Distance (Å)
				Amino Acid	Ligand	
17AAG	-11.5	-56.2	-18.3	TYR128	C21=O	2.48
GM	-8.1	-68.0	-15.5	TYR128	C21=O	2.50
17AG	-13.6	-56.1	-16.1	TYR128	C21=O	2.52
17DMAG	-12.0	-52.7	-12.7	TYR128	C21=O	2.54
17AEP-GA	-15.7	-39.4	-8.7	TYR128	C21=O	2.57

Table 1. Interaction and associated energies of the *trans*-amide isomers of the benzoquinone ansamycins in complex with NQO1. Where ΔV_{vdw} is van der Waals energy, ΔV_{elect} is electrostatic energy, and ΔG_{bind} is binding energy.

Molecular Pharmacology Fast Forward. Published on February 1, 2011 as DOI: 10.1124/mol.110.070086
This article has not been copyedited and formatted. The final version may differ from this version.

Compound	Dock Score	ΔV_{vdw} (kcal/mol)	ΔV_{elect} (kcal/mol)	ΔG_{bind} (kcal/mol)	H-Bond Interaction		H-Bond Distance (Å)
					Amino Acid	Ligand	
trans-17AAG	60.4	-10.5	-58.1	-16.2	SER113	C18=O	1.76
trans-17AAGH$_2$	86.2	-13.8	-75.6	-24.6	---	---	---
cis-17AAG	56.7	-15.3	-57.5	-26.9	PHE138	C1=O	2.26
					ASP54	C17-NHR^1	2.23
					LYS112	C21=O	1.80
					ASP93	C24-NH$_2$	1.91
cis-17AAGH$_2$	89.7	-12.9	-65.8	-34.9	PHE138	C1=O	2.14
					ASP54	C17-NHR^1	2.08
					ASP54	C18-OH	1.60
					LYS112	C21-OH	1.96
					ASP93	C24-NH$_2$	2.06

Table 2. Interactions and associated energies for the *trans*-/*cis*-amide isomers of 17AAG and 17AAGH$_2$ in complex with the open human Hsp90 structure. Where ΔV_{vdw} is van der Waals energy, ΔV_{elect} is electrostatic energy, and ΔG_{bind} is binding energy.

Molecular Pharmacology Fast Forward. Published on February 1, 2011 as DOI: 10.1124/mol.110.070086
This article has not been copyedited and formatted. The final version may differ from this version.

Compound	Dock Score	ΔV_{vdw} (kcal/mol)	ΔV_{elect} (kcal/mol)	ΔG_{bind} (kcal/mol)	H-Bond Interaction		H-Bond Distance (Å)
					Amino Acid	Ligand	
cis-17AAG	61.4	-12.2	-50.5	-13.4	PHE138	C1=O	2.04
					LYS58	C11-OH	1.88
					ASP54	C17-NHR[1]	2.37
					LYS112	C21=O	1.71
					ASP93	C24-NH_2	1.87
cis-17AAGH_2	88.3	-13.0	-64.9	-16.9	PHE138	C1=O	1.95
					LYS58	C11-OH	1.92
					ASP54	C17-NHR[1]	2.18
					ASP54	C18-OH	1.65
					LYS112	C21-OH	2.01
					ASP93	C24-NH_2	1.85

Table 3. Interactions and associated energies for the *cis*-amide isomers of 17AAG and 17AAGH_2 in complex with the bound human Hsp90 structure. Where ΔV_{vdw} is van der Waals energy, ΔV_{elect} is electrostatic energy, and ΔG_{bind} is binding energy.

Molecular Pharmacology Fast Forward. Published on February 1, 2011 as DOI: 10.1124/mol.110.070086
This article has not been copyedited and formatted. The final version may differ from this version.

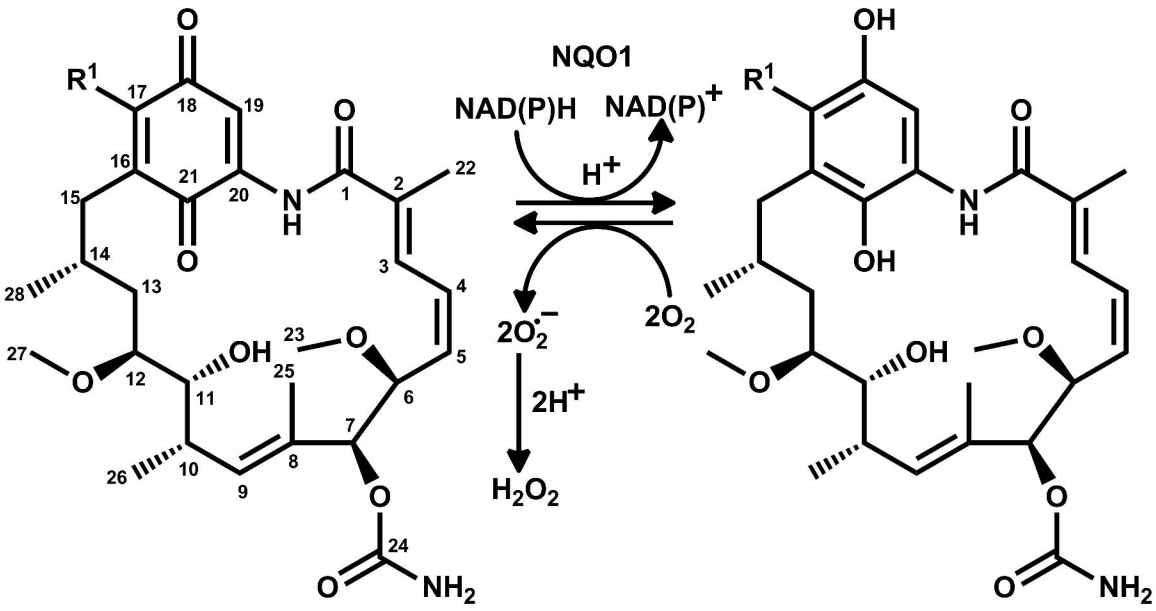

Compound	R^1 (17-Substituent)	MW
GM	OCH_3	560
17AAG	$NHCH_2CHCH_2$	586
17AG	NH_2	545
17DMAG	$NHCH_2CH_2N(CH_3)_2$	616
17AEP-GA	$NHCH_2CH_2NC_4H_8$	643

Scheme 1

Molecular Pharmacology Fast Forward. Published on February 1, 2011 as DOI: 10.1124/mol.110.070086
This article has not been copyedited and formatted. The final version may differ from this version.

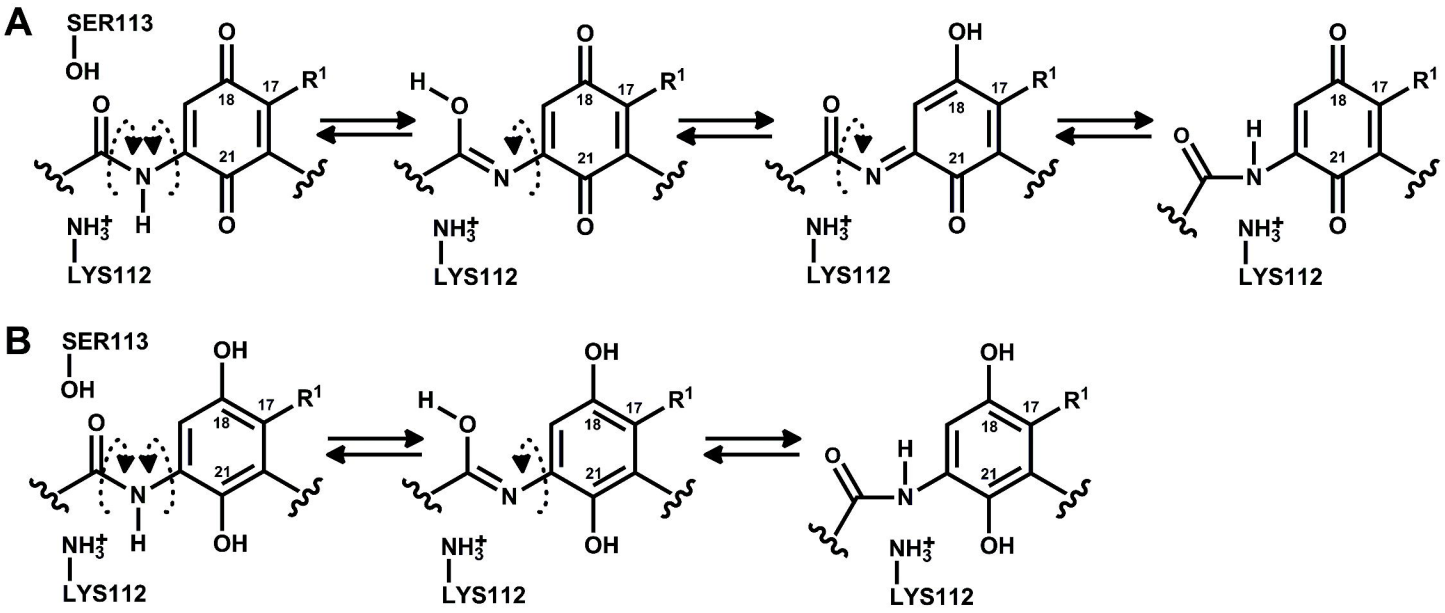

Scheme 2

Molecular Pharmacology Fast Forward. Published on February 1, 2011 as DOI: 10.1124/mol.110.070086
This article has not been copyedited and formatted. The final version may differ from this version.

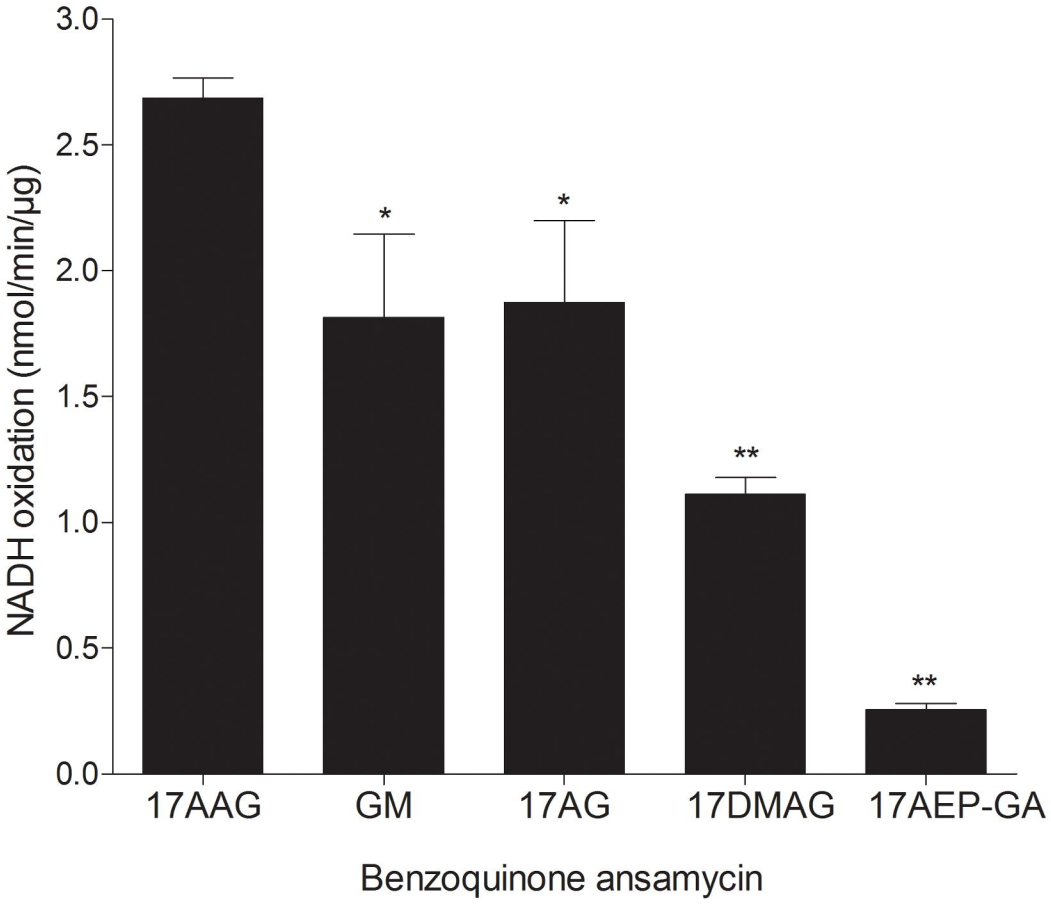

Figure 1

Molecular Pharmacology Fast Forward. Published on February 1, 2011 as DOI: 10.1124/mol.110.070086
This article has not been copyedited and formatted. The final version may differ from this version.

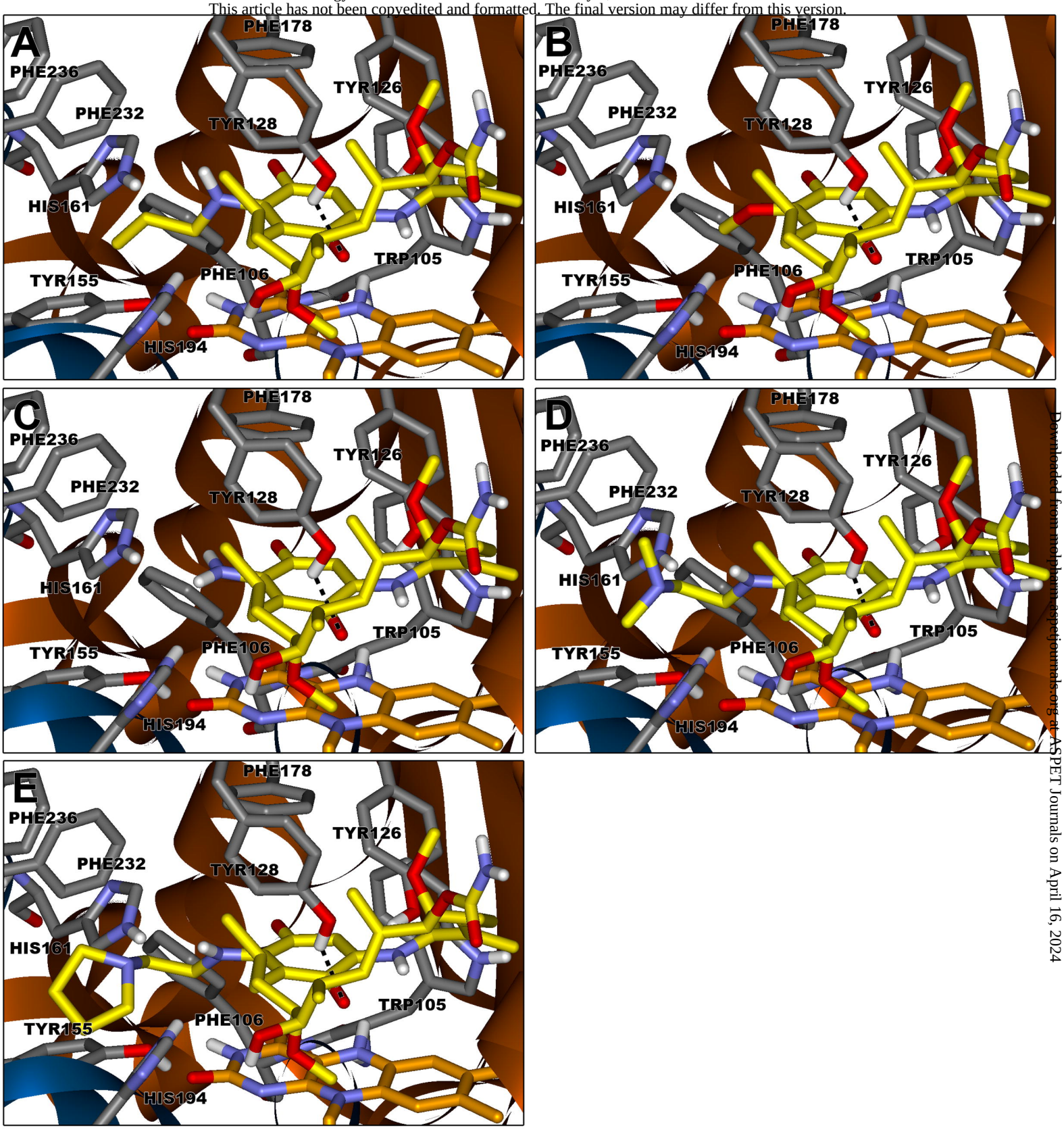

Figure 2

Molecular Pharmacology Fast Forward. Published on February 1, 2011 as DOI: 10.1124/mol.110.070086
This article has not been copyedited and formatted. The final version may differ from this version.

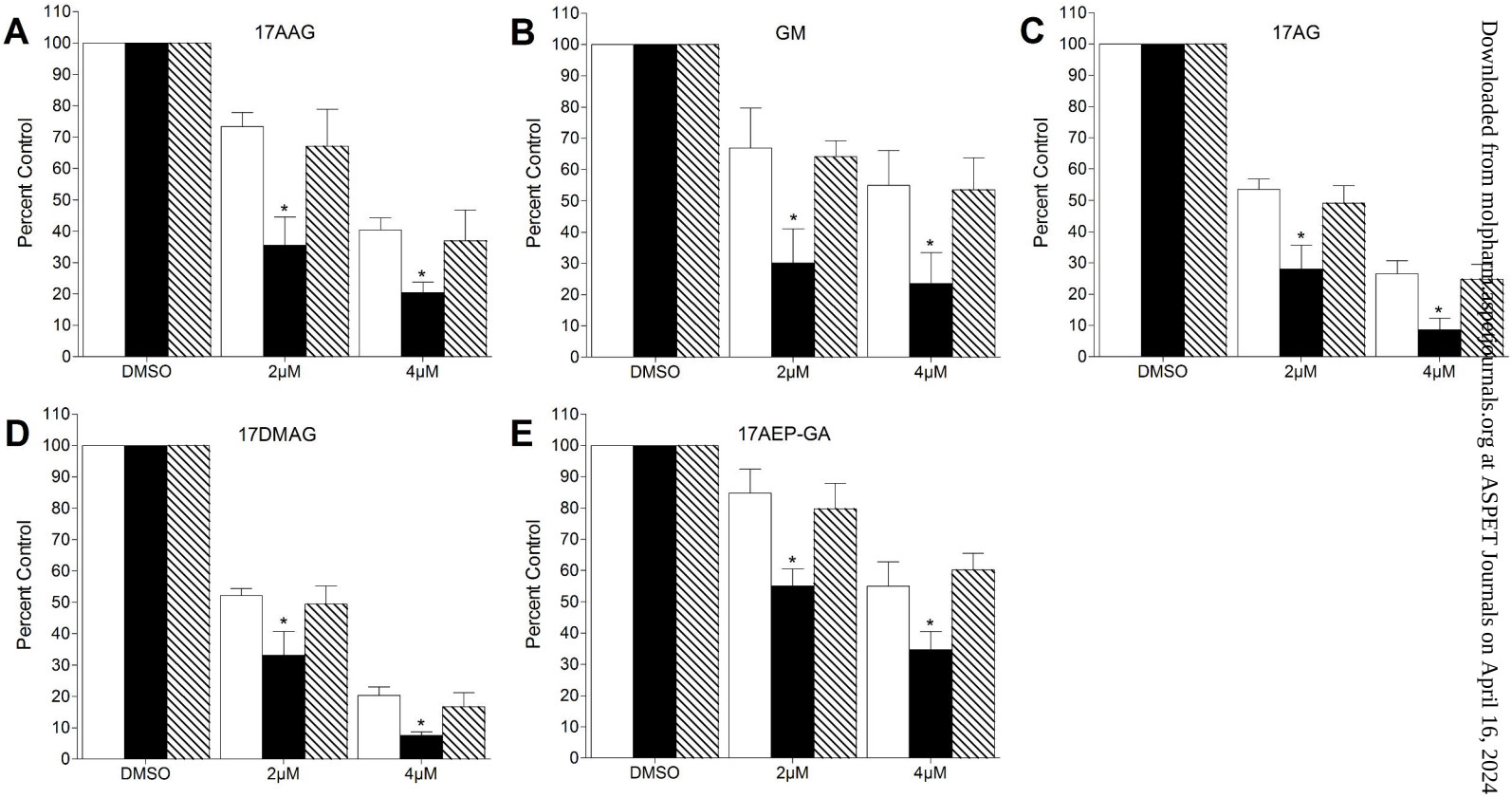

Figure 3

Molecular Pharmacology Fast Forward. Published on February 1, 2011 as DOI: 10.1124/mol.110.070086
This article has not been copyedited and formatted. The final version may differ from this version.

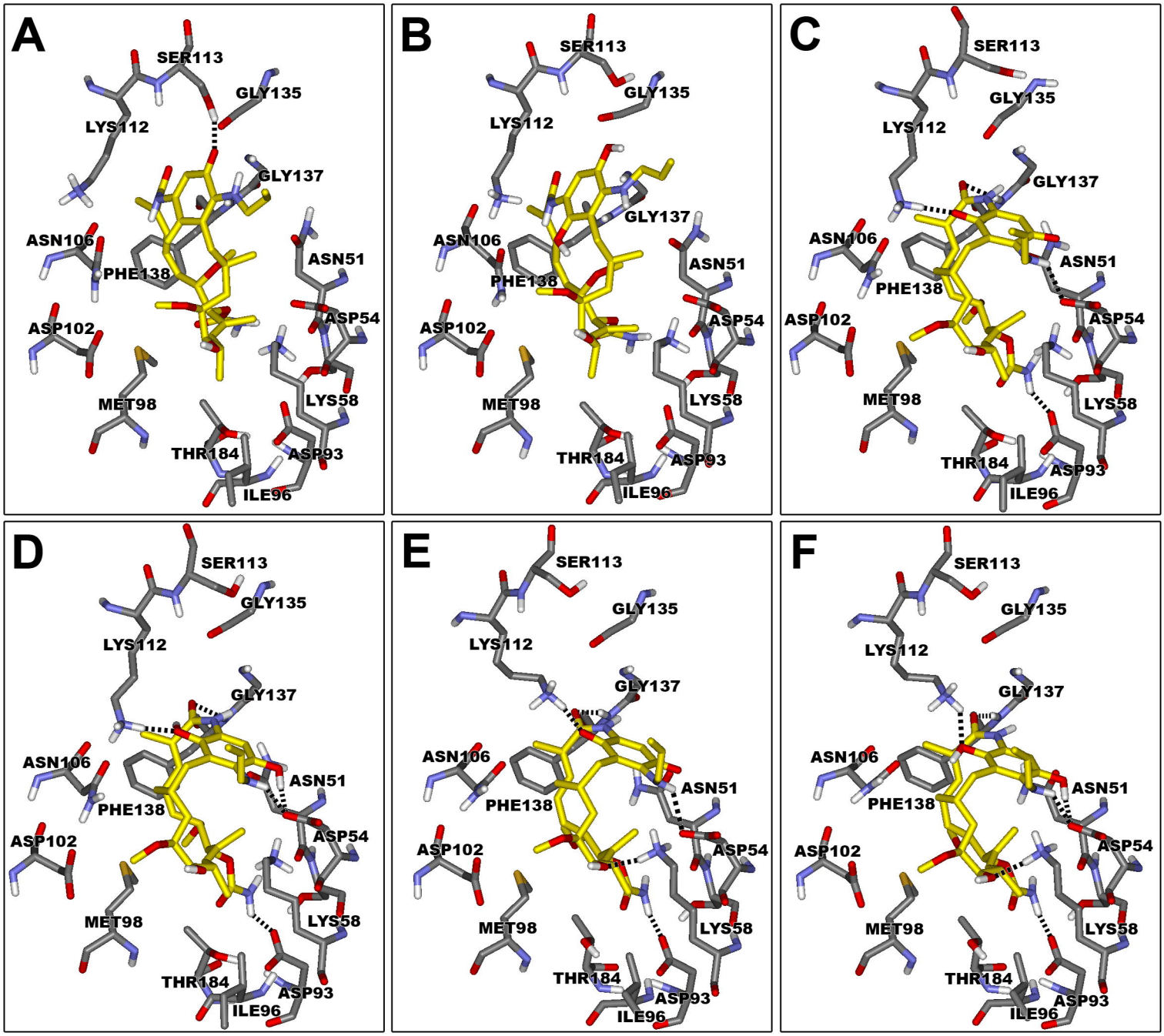

Figure 4

Molecular Pharmacology Fast Forward. Published on February 1, 2011 as DOI: 10.1124/mol.110.070086
This article has not been copyedited and formatted. The final version may differ from this version.

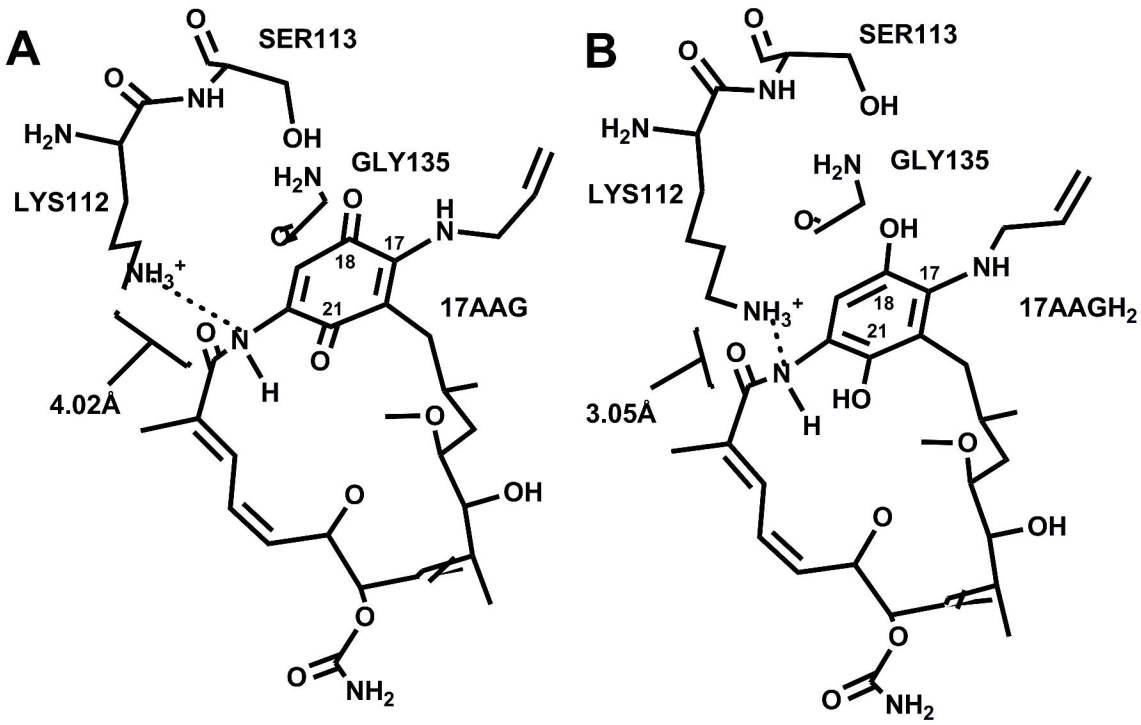

Figure 5

Supplemental Data: Molecular Pharmacology #070086

A Mechanistic and Structural Analysis of the Inhibition of Heat Shock Protein 90 by the Benzoquinone and Hydroquinone Ansamycins

Philip Reigan, David Siegel, Wenchang Guo, and David Ross

Department of Pharmaceutical Sciences, School of Pharmacy, University of Colorado Denver, Denver, Colorado 80045, USA.

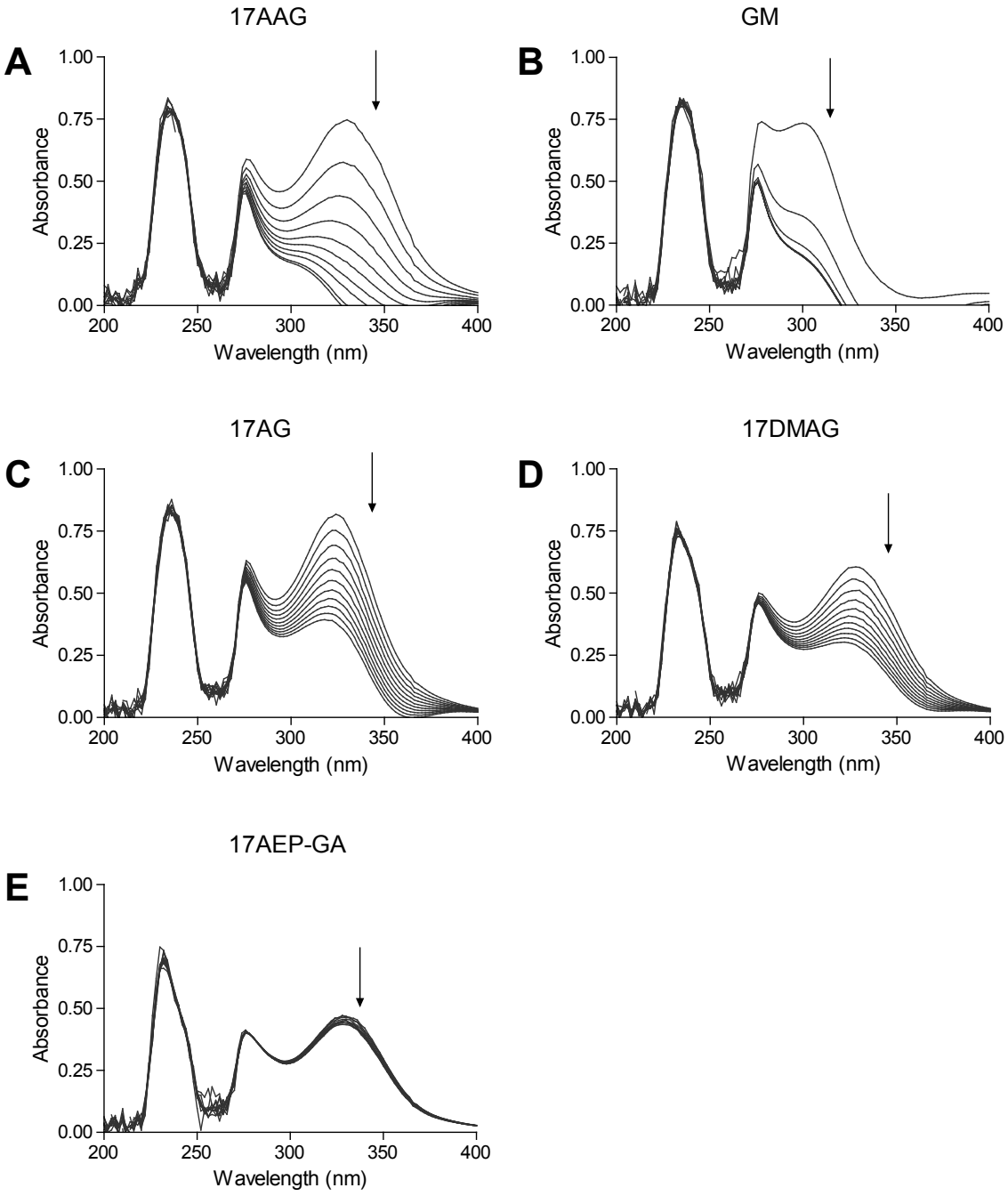

Figure 1.2 Spectrophotometric analysis of the NQO1-mediated reduction of the benzoquinone ansamycins.

Spectrophotometric analysis of the reduction of the benzoquinone ansamycins A) 17AAG, B) GM, C) 17AG, D) 17DMAG, and E) 17AEP-GA by rhNQO1. Reaction conditions: 50 μM benzoquinone ansamycin, 200 μM NADH, and rhNQO1 (6.6 μg; except for 17AAG 3.3 μg) incubated in 50 mM potassium phosphate buffer (pH 7.4, 1 mL) at room temperature. The absorbance changes during the reduction of benzoquinone ansamycin by rhNQO1 were monitored spectrophotometrically every 30 sec over 5 min. Reactions in the absence of rhNQO1 were used as controls.

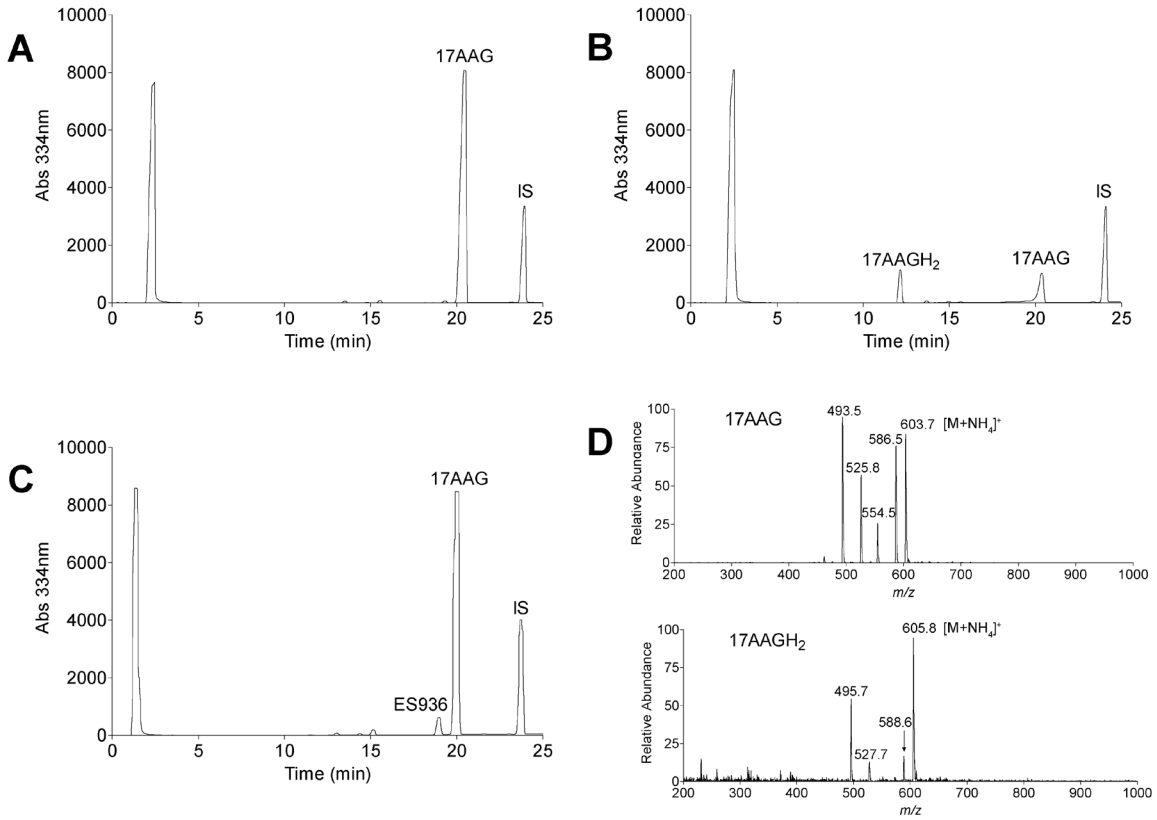

Figure 2.1 HPLC and LC-MS analysis of the reduction of 17AAG by purified rhNQO1 to $17AAGH_2$.

HPLC analysis of the rhNQO1-mediated reduction of A) 17AAG to B) $17AAGH_2$ and inhibition of this reduction by C) ES936. A) 17AAG and NADH; B) 17AAG, NADH, and rhNQO1; C) 17AAG, NADH, rhNQO1, and ES936 (1 μM). Reaction conditions: 50 μM 17AAG, 500 μM NADH, and 3.3 μg rhNQO1 in 50 mM potassium phosphate buffer (pH 7.4, 1 mL). After 40 min reactions were stopped with an equal volume of acetonitrile containing internal standard N-phenyl-1-naphthylamine (5 μg/mL), centrifuged and the supernatant was analyzed immediately by HPLC at 334 nm. D) LC-MS confirmed $17AAGH_2$ as the product of NQO1-mediated reduction of 17AAG.

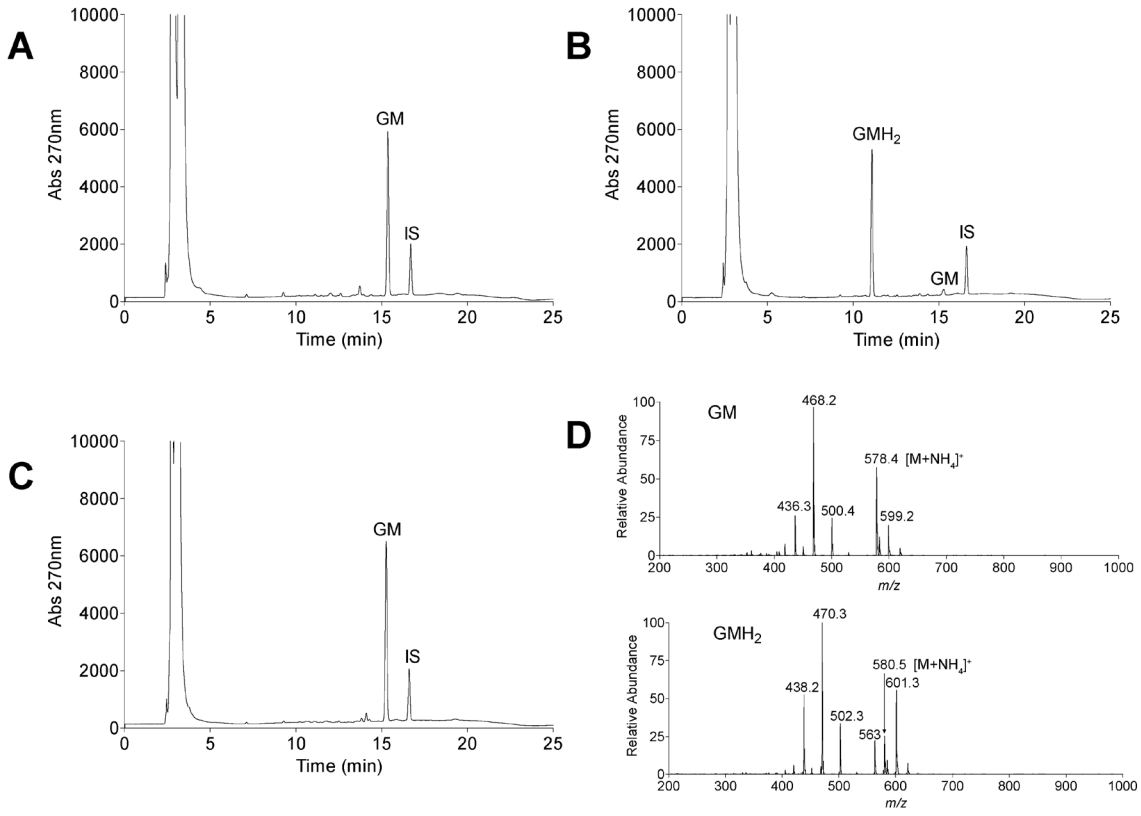

Figure 2.2. HPLC and LC-MS analysis of the reduction of GM by purified rhNQO1 to GMH_2.

HPLC analysis of the rhNQO1-mediated reduction of A) GM to B) GMH_2 and inhibition of this reduction by C) ES936. A) GM and NADH; B) GM, NADH, and rhNQO1; C) GM, NADH, rhNQO1, and ES936 (1 μM). Reaction conditions: 20 μM GM, 500 μM NADH, and 6.6 μg rhNQO1 in 50 mM potassium phosphate buffer (pH 7.4, 1 mL). After 30 min reactions were stopped with an equal volume of acetonitrile containing internal standard N-phenyl-1-naphthylamine (10 μg/mL), centrifuged and the supernatant was analyzed immediately by HPLC at 270 nm. D) LC-MS confirmed GMH_2 as the product of NQO1-mediated reduction of GM.

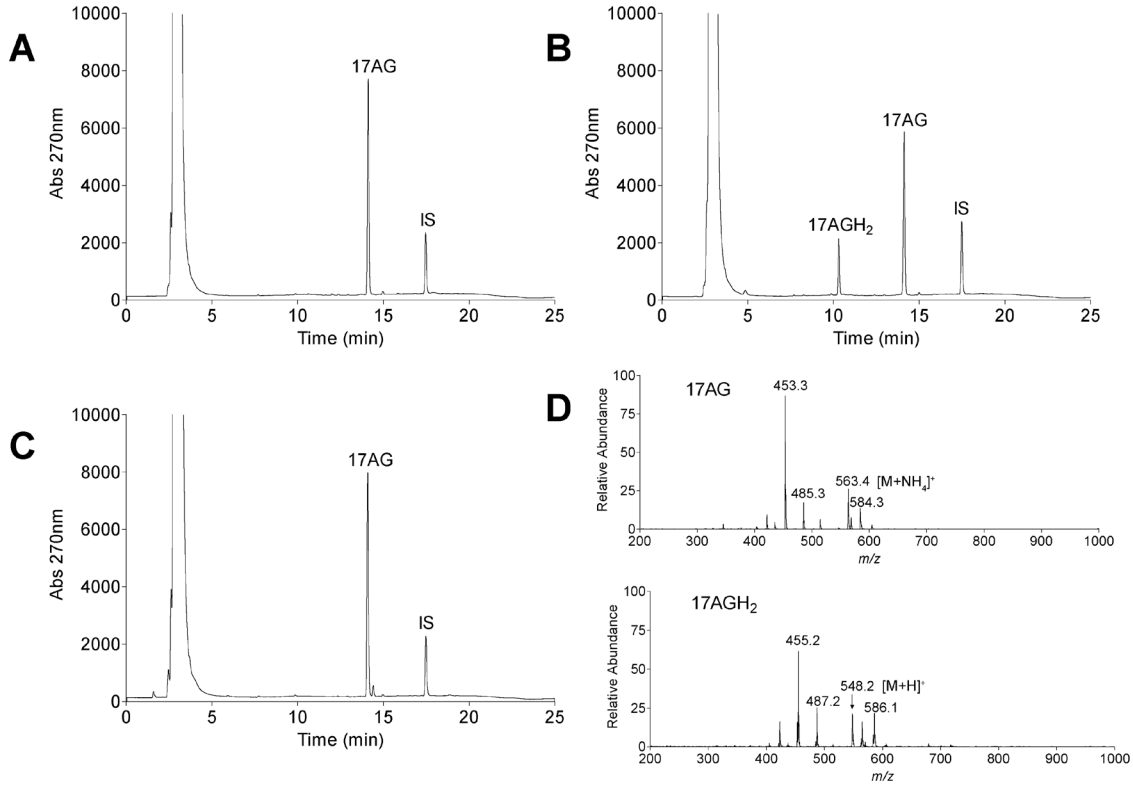

Figure 2.3. HPLC and LC-MS analysis of the reduction of 17AG by purified rhNQO1 to $17AGH_2$.

HPLC analysis of the rhNQO1-mediated reduction of A) 17AG to B) $17AGH_2$ and inhibition of this reduction by C) ES936. A) 17AG and NADH; B) 17AG, NADH, and rhNQO1; C) 17AG, NADH, rhNQO1, and ES936 (1 μM). Reaction conditions: 20 μM 17AG, 500 μM NADH, and 6.6 μg rhNQO1 in 50 mM potassium phosphate buffer (pH 7.4, 1 mL). After 30 min reactions were stopped with an equal volume of acetonitrile containing internal standard N-phenyl-1-naphthylamine (10 μg/mL), centrifuged and the supernatant was analyzed immediately by HPLC at 270 nm. D) LC-MS confirmed $17AGH_2$ as the product of NQO1-mediated reduction of 17AG.

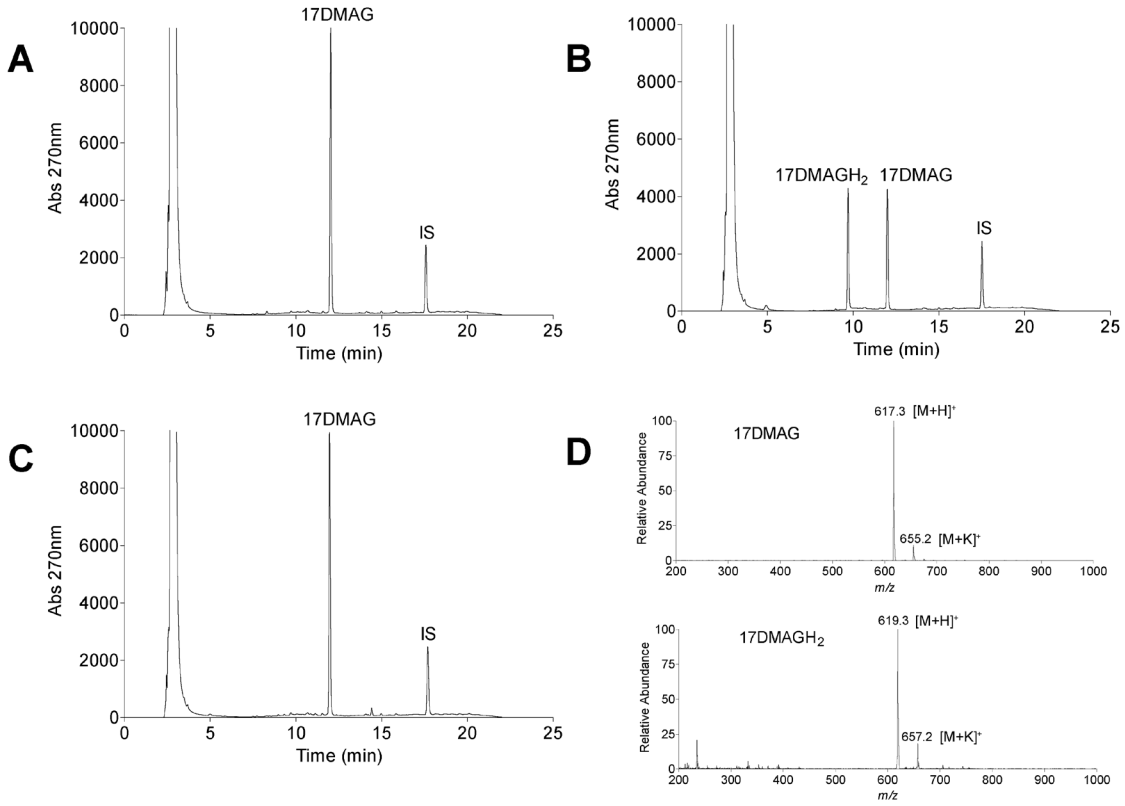

Figure 2.4. HPLC and LC-MS analysis of the reduction of 17DMAG by purified rhNQO1 to $17DMAGH_2$.

HPLC analysis of the rhNQO1-mediated reduction of A) 17DMAG to B) $17DMAGH_2$ and inhibition of this reduction by C) ES936. A) 17DMAG and NADH; B) 17DMAG, NADH, and rhNQO1; C) 17DMAG, NADH, rhNQO1, and ES936 (1 μM). Reaction conditions: 20 μM 17DMAG, 500 μM NADH, and 6.6 μg rhNQO1 in 50 mM potassium phosphate buffer (pH 7.4, 1 mL). After 30 min reactions were stopped with an equal volume of acetonitrile containing internal standard N-phenyl-1-naphthylamine (10 μg/mL), centrifuged and the supernatant was analyzed immediately by HPLC at 270 nm. D) LC-MS confirmed $17DMAGH_2$ as the product of NQO1-mediated reduction of 17DMAG.

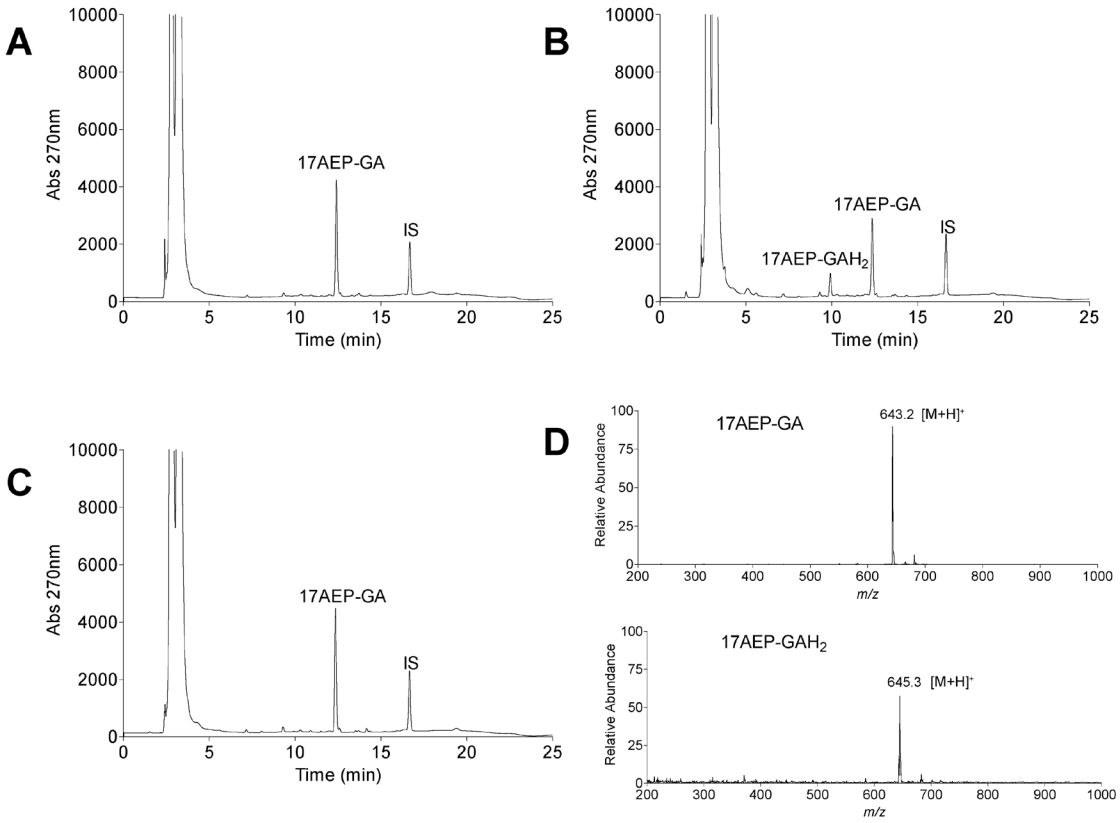

Figure 2.5. HPLC and LC-MS analysis of the reduction of 17AEP-GA by purified rhNQO1 to 17AEP-GAH_2.

HPLC analysis of the rhNQO1-mediated reduction of A) 17AEP-GA to B) 17AEP-GAH_2 and inhibition of this reduction by C) ES936. A) 17AEP-GA and NADH; B) 17AEP-GA, NADH, and rhNQO1; C) 17AEP-GA, NADH, rhNQO1, and ES936 (1 μM). Reaction conditions: 20 μM 17AEP-GA, 500 μM NADH, and 16.5 μg rhNQO1 in 50 mM potassium phosphate buffer (pH 7.4, 1 mL). After 30 min reactions were stopped with an equal volume of acetonitrile containing internal standard N-phenyl-1-naphthylamine (10 μg/mL), centrifuged and the supernatant was analyzed immediately by HPLC at 270 nm. D) LC-MS confirmed 17AEP-GAH_2 as the product of NQO1-mediated reduction of 17AEP-GA.

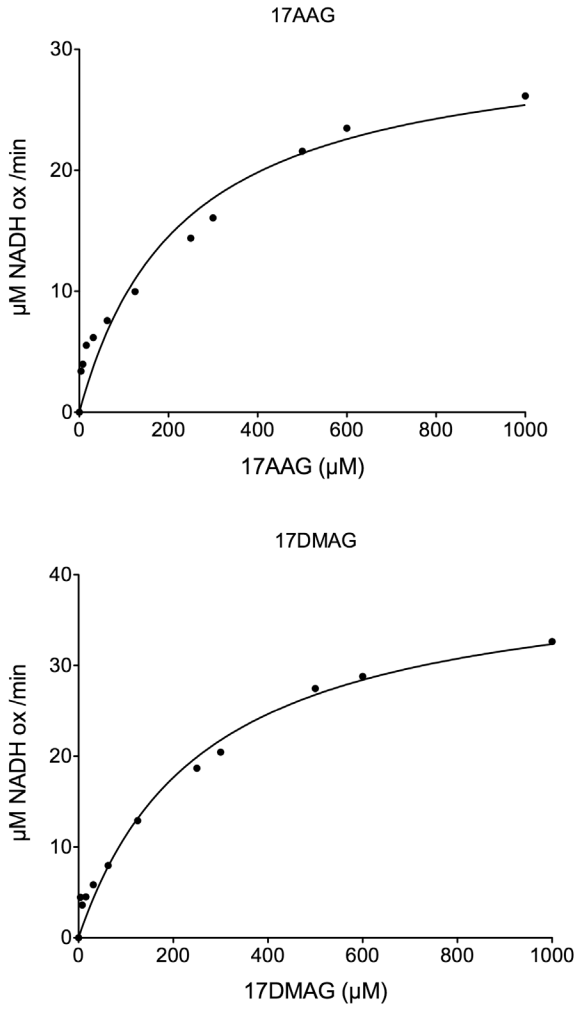

Figure 3. Kinetic saturation curves for the reduction of 17AAG and 17DMAG by NQO1.

Enzyme velocity as a function of benzoquinone ansamycin concentration was determined by measuring NQO1-dependent NADH oxidation using fluorescent spectroscopy as described in the *Experimental Section*.

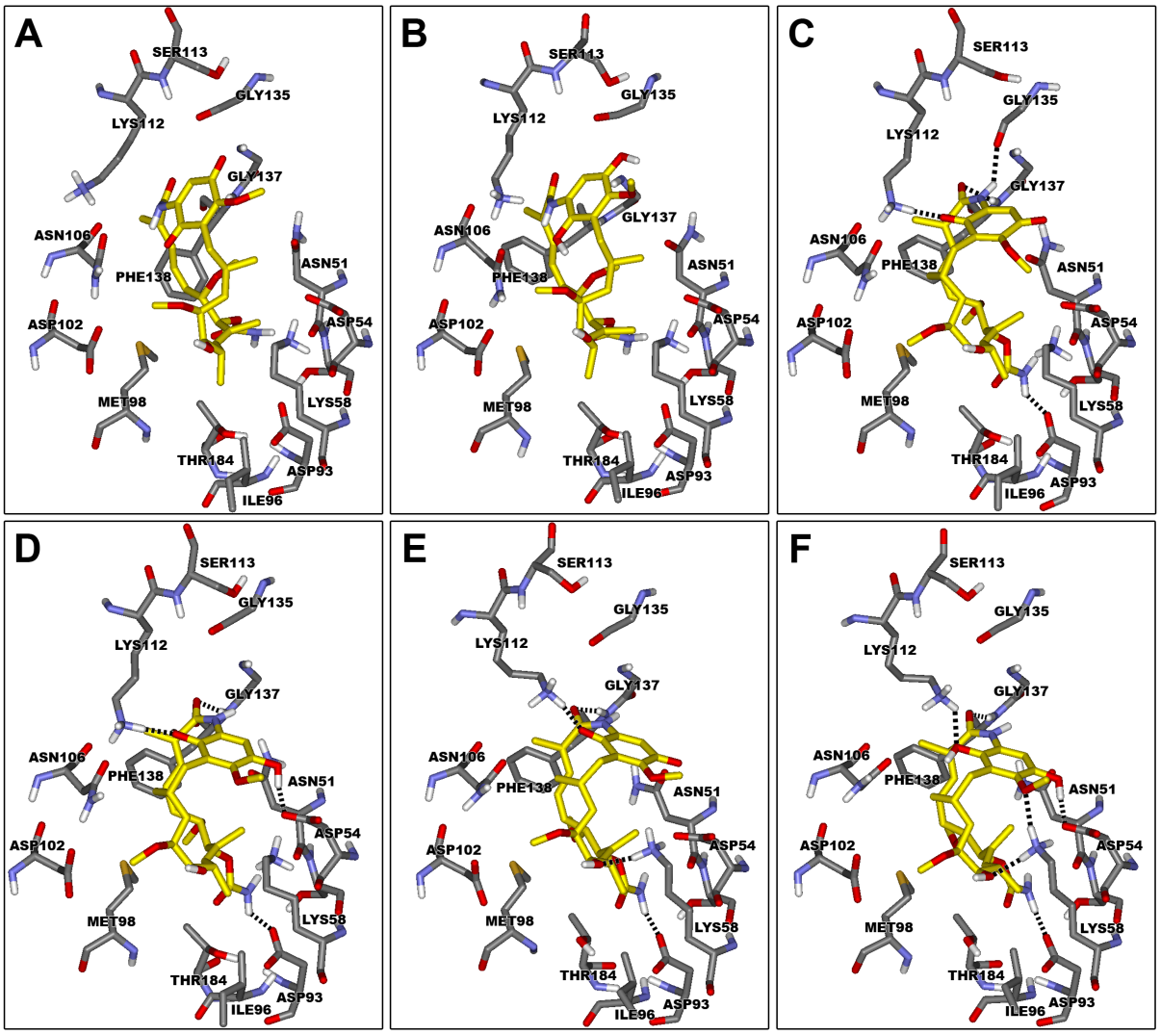

Figure 4.2. The human Hsp90-GM/GMH_2 complex.

The nucleotide-binding domain of open human Hsp90 in complex with the *trans*-amide isomer of A) GM and B) GMH_2 and the *cis*-amide isomer of C) GM and D) GMH_2. The nucleotide-binding domain of bound human Hsp90 in complex with the *cis*-amide isomer of E) GM and F) GMH_2. GM and GMH_2 (stick display style; carbon atoms colored yellow) in the nucleotide-binding domain of Hsp90, key amino acid residues (stick display style; colored by atom type), and hydrogen bond interactions (black dashed lines) are displayed.

Compound	Dock Score	ΔV_{vdw} (kcal/mol)	ΔV_{elect} (kcal/mol)	ΔG_{bind} (kcal/mol)	H-Bond Interaction		H-Bond Distance (Å)
					Amino Acid	Ligand	
trans-GM	41.3	-7.7	-63.3	-20.8	---	---	---
trans-GMH_2	79.5	-10.1	-61.8	-30.5	---	---	---
cis-GM	43.2	-9.9	-63.0	-23.7	GLY135	C1-N<u>H</u>	2.40
					PHE138	C1=<u>O</u>	2.26
					LYS112	C21=<u>O</u>	1.72
					ASP93	C24-N<u>H_2</u>	1.99
cis-GMH_2	80.7	-10.9	-63.0	-38.6	PHE138	C1=<u>O</u>	2.12
					ASP54	C18-O<u>H</u>	1.59
					LYS112	C21-<u>O</u>H	1.86
					ASP93	C24-N<u>H_2</u>	2.06

Table 1.2. Interaction energies and hydrogen bond interactions for the *trans*-/*cis*-amide isomers of GM and GMH_2 in complex with the open human Hsp90 structure.

Where ΔV_{vdw} is van der Waals energy, ΔV_{elect} is electrostatic energy, and ΔG_{bind} is binding energy.

Compound	Dock Score	ΔV_{vdw} (kcal/mol)	ΔV_{elect} (kcal/mol)	ΔG_{bind} (kcal/mol)	H-Bond Interaction		H-Bond Distance (Å)
					Amino Acid	Ligand	
cis-GM	45.8	-9.2	-49.2	-13.5	PHE138	C1=<u>O</u>	2.04
					LYS58	C11-<u>O</u>H	1.84
					LYS112	C21=<u>O</u>	1.70
					ASP93	C24-N<u>H_2</u>	1.89
cis-GMH_2	81.2	-16.6	-58.8	-19.1	PHE138	C1=<u>O</u>	1.96
					LYS58	C11-<u>O</u>H	1.95
					LYS58	C17-<u>O</u>R^1	2.21
					ASP54	C18-O<u>H</u>	1.65
					LYS112	C21-<u>O</u>H	2.10
					ASP93	C24-N<u>H_2</u>	1.88

Table 2.2. Interaction energies and hydrogen bond interactions for the *cis*-amide isomers of GM and GMH_2 in complex with the bound human Hsp90 structure.

Where ΔV_{vdw} is van der Waals energy, ΔV_{elect} is electrostatic energy, and ΔG_{bind} is binding energy.

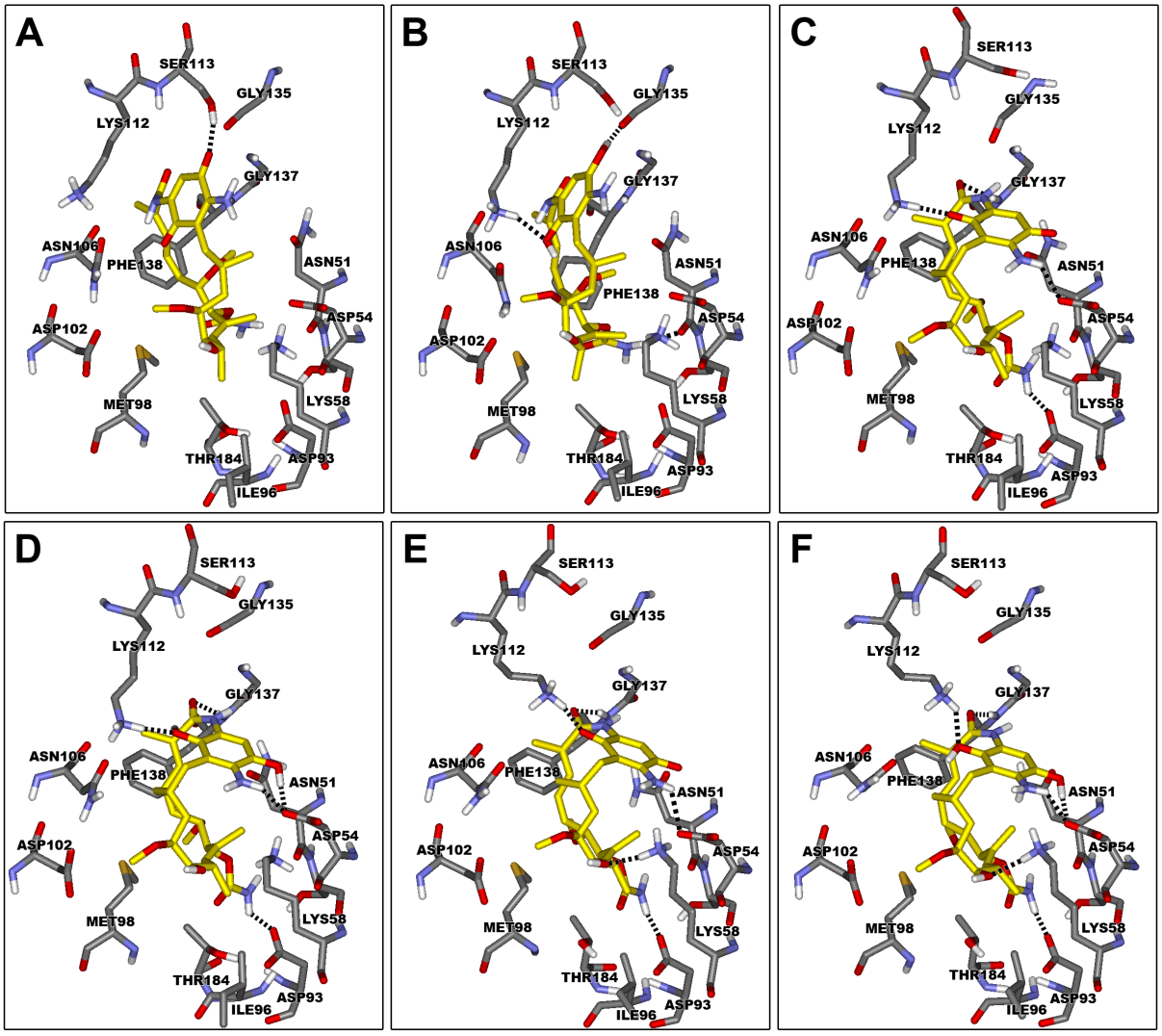

Figure 4.3. The human Hsp90-17AG/17AGH$_2$ complex.

The nucleotide-binding domain of open human Hsp90 in complex with the *trans*-amide isomer of A) 17AG and B) 17AGH$_2$ and the *cis*-amide isomer of C) 17AG and D) 17AGH$_2$. The nucleotide-binding domain of bound human Hsp90 in complex with the *cis*-amide isomer of E) 17AG and F) 17AGH$_2$. 17AG and 17AGH$_2$ (stick display style; carbon atoms colored yellow) in the nucleotide-binding domain of Hsp90, key amino acid residues (stick display style; colored by atom type), and hydrogen bond interactions (black dashed lines) are displayed.

Compound	Dock Score	ΔV_{vdw} (kcal/mol)	ΔV_{elect} (kcal/mol)	ΔG_{bind} (kcal/mol)	H-Bond Interaction		H-Bond Distance (Å)
					Amino Acid	Ligand	
trans-17AG	60.1	-13.7	-56.0	-16.0	SER113	C18=O	1.76
trans-17AGH$_2$	88.8	-8.2	-73.9	-36.8	GLY135	C18-OH	1.67
					ASN51	C24-NH$_2$	2.42
cis-17AG	61.2	-15.6	-55.7	-15.5	PHE138	C1=O	2.28
					ASP54	C17-NH$_2$	2.22
					LYS112	C21=O	1.78
					ASP93	C24-NH$_2$	1.95
cis-17AGH$_2$	90.0	-8.2	--73.9	-33.9	PHE138	C1=O	2.12
					ASP54	C17-NH$_2$	2.17
					ASP54	C18-OH	1.61
					LYS112	C21-OH	1.90
					ASP93	C24-NH$_2$	2.16

Table 1.3. Interaction energies and hydrogen bond interactions for the *trans*-/*cis*-amide isomers of 17AG and 17AGH$_2$ in complex with the open human Hsp90 structure.

Where ΔV_{vdw} is van der Waals energy, ΔV_{elect} is electrostatic energy, and ΔG_{bind} is binding energy.

Compound	Dock Score	ΔV_{vdw} (kcal/mol)	ΔV_{elect} (kcal/mol)	ΔG_{bind} (kcal/mol)	H-Bond Interaction		H-Bond Distance (Å)
					Amino Acid	Ligand	
cis-17AG	62.2	-15.3	-56.2	-12.5	PHE138	C1=O	2.08
					LYS58	C11-OH	1.89
					LYS112	C21=O	1.70
					ASP93	C24-NH$_2$	1.84
cis-17AGH$_2$	88.2	-10.4	-70.0	-17.2	PHE138	C1=O	1.98
					LYS58	C11-OH	1.99
					ASP54	C17-NHR^1	2.29
					ASP54	C18-OH	1.61
					LYS112	C21-OH	2.03
					ASP93	C24-NH$_2$	1.86

Table 2.3. Interaction energies and hydrogen bond interactions for the *cis*-amide isomers of 17AG and 17AGH$_2$ in complex with the bound human Hsp90 structure.

Where ΔV_{vdw} is van der Waals energy, ΔV_{elect} is electrostatic energy, and ΔG_{bind} is binding energy.

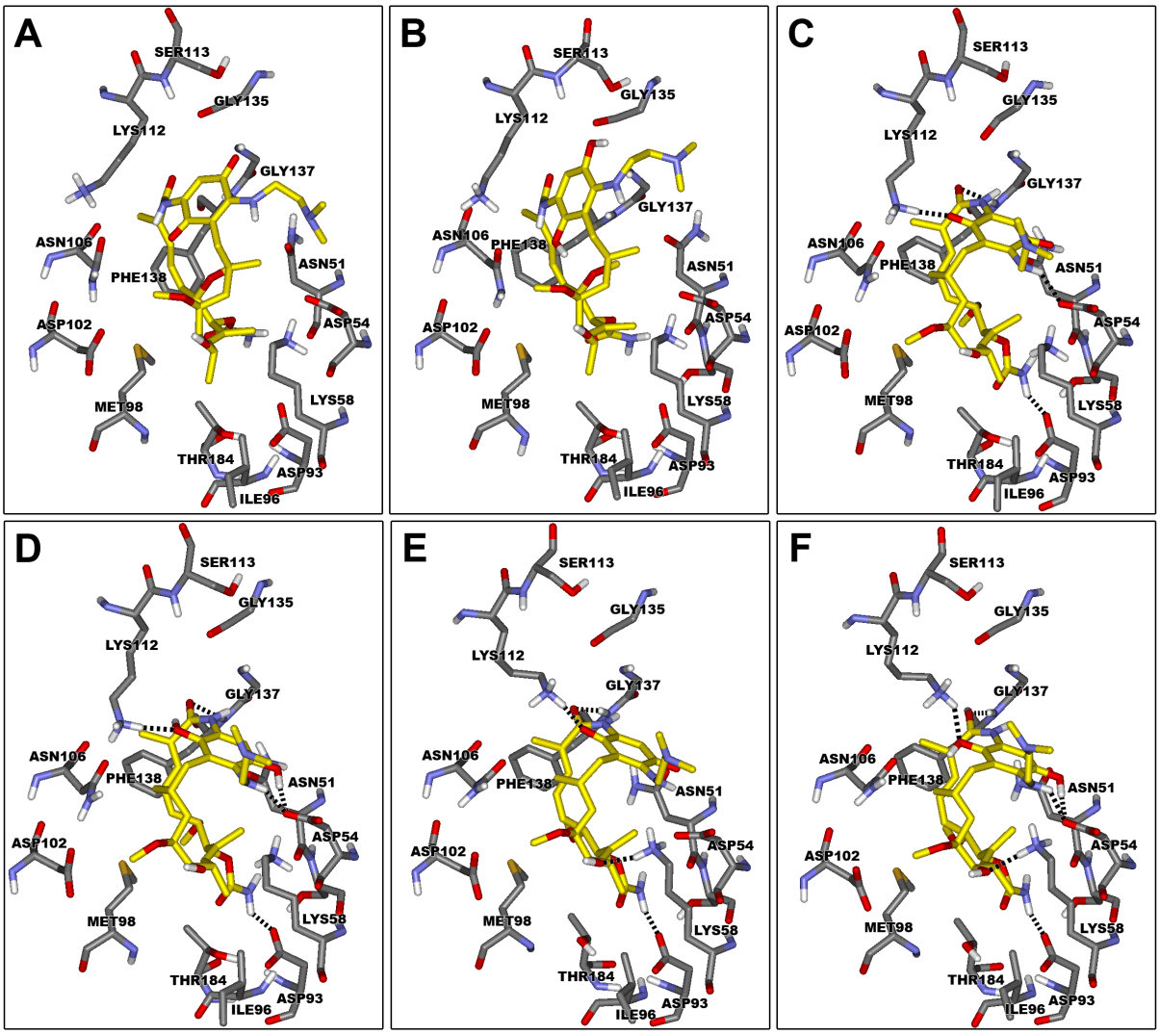

Figure 4.4. The human Hsp90-17DMAG/17DMAGH$_2$ complex.

The nucleotide-binding domain of open human Hsp90 in complex with the *trans*-amide isomer of A) 17DMAG and B) 17DMAGH$_2$ and the *cis*-amide isomer of C) 17DMAG and D) 17DMAGH$_2$. The nucleotide-binding domain of bound human Hsp90 in complex with the *cis*-amide isomer of E) 17DMAG and F) 17DMAGH$_2$. 17DMAG and 17DMAGH$_2$ (stick display style; carbon atoms colored yellow) in the nucleotide-binding domain of Hsp90, key amino acid residues (stick display style; colored by atom type), and hydrogen bond interactions (black dashed lines) are displayed.

Compound	Dock Score	ΔV_{vdw} (kcal/mol)	ΔV_{elect} (kcal/mol)	ΔG_{bind} (kcal/mol)	H-Bond Interaction		H-Bond Distance (Å)
					Amino Acid	Ligand	
trans-17DMAG	29.8	-13.2	-48.0	-29.3	---	---	---
trans-17DMAGH$_2$	73.1	-7.0	-75.1	-30.6	---	---	---
cis-17DMAG	30.4	-13.1	-49.4	-29.6	PHE138	C1=O	2.24
					ASP54	C17-NHR^1	2.05
					LYS112	C21=O	1.77
					ASP93	C24-NH$_2$	1.89
cis-17DMAGH$_2$	82.3	-16.2	-59.1	-29.8	PHE138	C1=O	2.16
					ASP54	C17-NHR^1	1.94
					ASP54	C18-OH	1.55
					LYS112	C21-OH	2.00
					ASP93	C24-NH$_2$	2.04

Table 1.4. Interaction energies and hydrogen bond interactions for the *trans*-/*cis*-amide isomers of 17DMAG and 17DMAGH$_2$ in complex with the open human Hsp90 structure.

Where ΔV_{vdw} is van der Waals energy, ΔV_{elect} is electrostatic energy, and ΔG_{bind} is binding energy.

Compound	Dock Score	ΔV_{vdw} (kcal/mol)	ΔV_{elect} (kcal/mol)	ΔG_{bind} (kcal/mol)	H-Bond Interaction		H-Bond Distance (Å)
					Amino Acid	Ligand	
cis-17DMAG	34.7	-9.6	-45.7	-11.1	PHE138	C1=O	2.10
					LYS58	C11-OH	1.89
					LYS112	C21=O	1.69
					ASP93	C24-NH$_2$	1.88
cis-17DMAGH$_2$	80.7	--16.0	-69.7	-16.0	PHE138	C1=O	1.99
					LYS58	C11-OH	1.96
					ASP54	C17-NHR^1	2.12
					ASP54	C18-OH	1.63
					LYS112	C21-OH	2.01
					ASP93	C24-NH$_2$	1.89

Table 2.4. Interaction energies and hydrogen bond interactions for the *cis*-amide isomers of 17DMAG and 17DMAGH$_2$ in complex with the bound human Hsp90 structure.

Where ΔV_{vdw} is van der Waals energy, ΔV_{elect} is electrostatic energy, and ΔG_{bind} is binding energy.

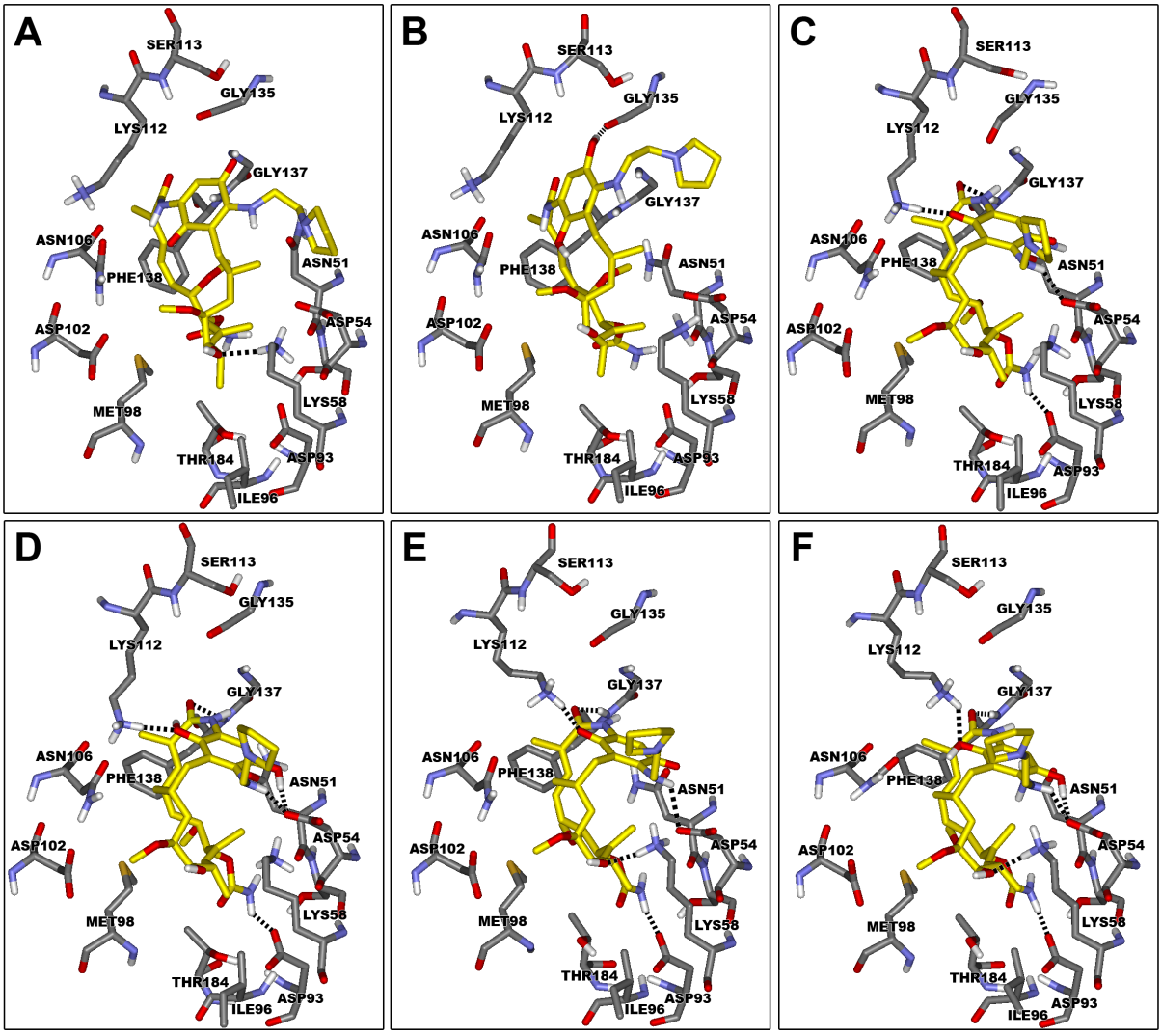

Figure 4.5. The human Hsp90-17AEP-GA/17AEP-GAH$_2$ complex.

The nucleotide-binding domain of open human Hsp90 in complex with the *trans*-amide isomer of A) 17AEP-GA and B) 17AEP-GAH$_2$ and the *cis*-amide isomer of C) 17AEP-GA and D) 17AEP-GAH$_2$. The nucleotide-binding domain of bound human Hsp90 in complex with the *cis*-amide isomer of E) 17AEP-GA and F) 17AEPGAH$_2$. 17AEP-GA and 17AEP-GAH$_2$ (stick display style; carbon atoms colored yellow) in the nucleotide-binding domain of Hsp90, key amino acid residues (stick display style; colored by atom type), and hydrogen bond interactions (black dashed lines) are displayed.

Compound	Dock Score	ΔV_{vdw} (kcal/mol)	ΔV_{elect} (kcal/mol)	ΔG_{bind} (kcal/mol)	H-Bond Interaction		H-Bond Distance (Å)
					Amino Acid	Ligand	
trans-17AEP-GA	13.3	-17.7	-55.3	-23.0	LYS58	C11-OH	2.23
trans-17AEP-GAH_2	79.5	-14.2	-75.0	-40.3	GLY135	C18-OH	1.65
cis-17AEP-GA	12.6	-15.7	-57.3	-27.9	PHE138	C1=O	2.16
					ASP54	C17-NHR[1]	2.05
					LYS112	C21=O	1.77
					ASP93	C24-NH_2	1.89
cis-17AEP-GAH_2	77.3	-18.5	-71.4	-29.4	PHE138	C1=O	2.15
					ASP54	C17-NHR[1]	1.94
					ASP54	C18-OH	1.55
					LYS112	C21-OH	2.04
					ASP93	C24-NH_2	2.04

Table 1.5. Interaction energies and hydrogen bond interactions for the *trans*-/*cis*-amide isomers of 17AEP-GA and 17AEPGAH_2 in complex with the open human Hsp90 structure.

Where ΔV_{vdw} is van der Waals energy, ΔV_{elect} is electrostatic energy, and ΔG_{bind} is binding energy.

Compound	Dock Score	ΔV_{vdw} (kcal/mol)	ΔV_{elect} (kcal/mol)	ΔG_{bind} (kcal/mol)	H-Bond Interaction		H-Bond Distance (Å)
					Amino Acid	Ligand	
cis-17AEP-GA	13.9	-18.8	-53.1	-10.3	PHE138	C1=O	2.06
					LYS58	C11-OH	1.87
					ASP54	C17-NHR[1]	2.47
					LYS112	C21=O	1.68
					ASP93	C24-NH_2	1.88
cis-17AEP-GAH_2	79.3	-14.2	-72.1	-14.4	PHE138	C1=O	2.00
					LYS58	C11-OH	1.96
					ASP54	C17-NHR[1]	2.20
					ASP54	C18-OH	1.62
					LYS112	C21-OH	2.06
					ASP93	C24-NH_2	1.82

Table 2.5. Interaction energies and hydrogen bond interactions for the *cis*-amide isomers of 17AEP-GA and 17AEP-GAH_2 in complex with the bound human Hsp90 structure.

Where ΔV_{vdw} is van der Waals energy, ΔV_{elect} is electrostatic energy, and ΔG_{bind} is binding energy.

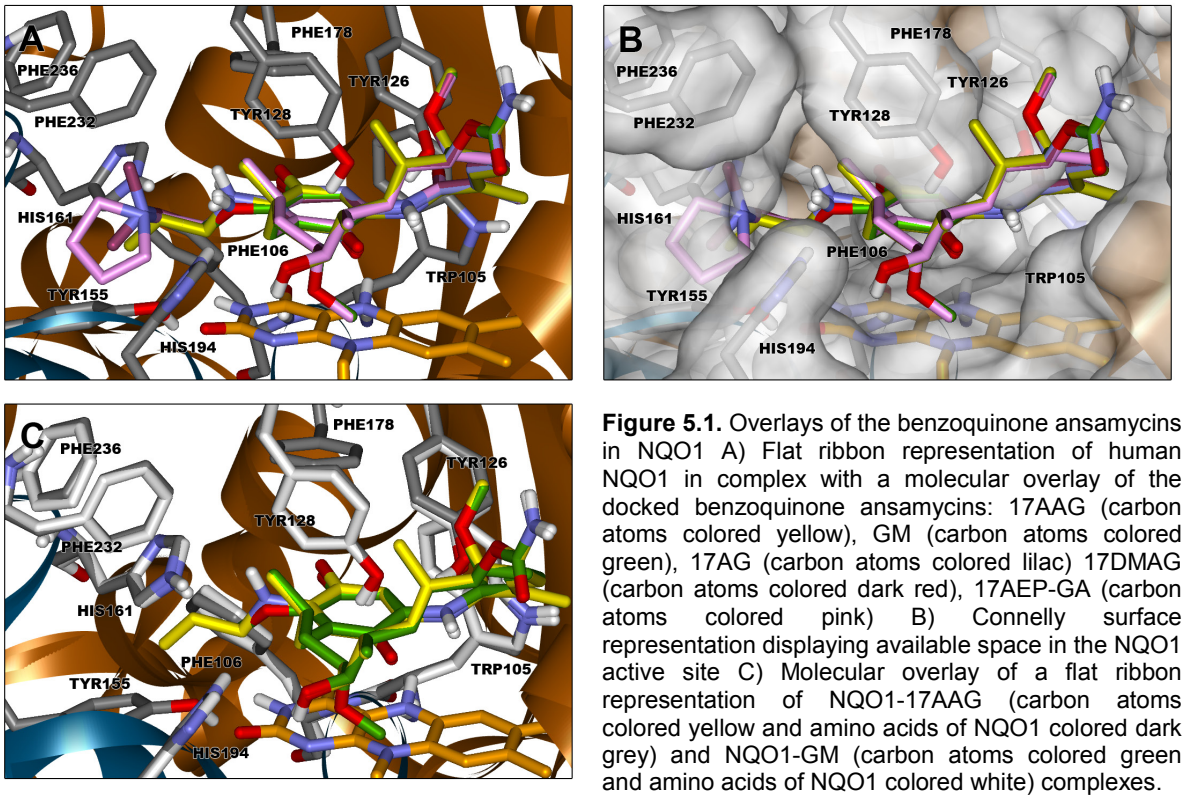

Figure 5.1. Overlays of the benzoquinone ansamycins in NQO1 A) Flat ribbon representation of human NQO1 in complex with a molecular overlay of the docked benzoquinone ansamycins: 17AAG (carbon atoms colored yellow), GM (carbon atoms colored green), 17AG (carbon atoms colored lilac) 17DMAG (carbon atoms colored dark red), 17AEP-GA (carbon atoms colored pink) B) Connelly surface representation displaying available space in the NQO1 active site C) Molecular overlay of a flat ribbon representation of NQO1-17AAG (carbon atoms colored yellow and amino acids of NQO1 colored dark grey) and NQO1-GM (carbon atoms colored green and amino acids of NQO1 colored white) complexes.

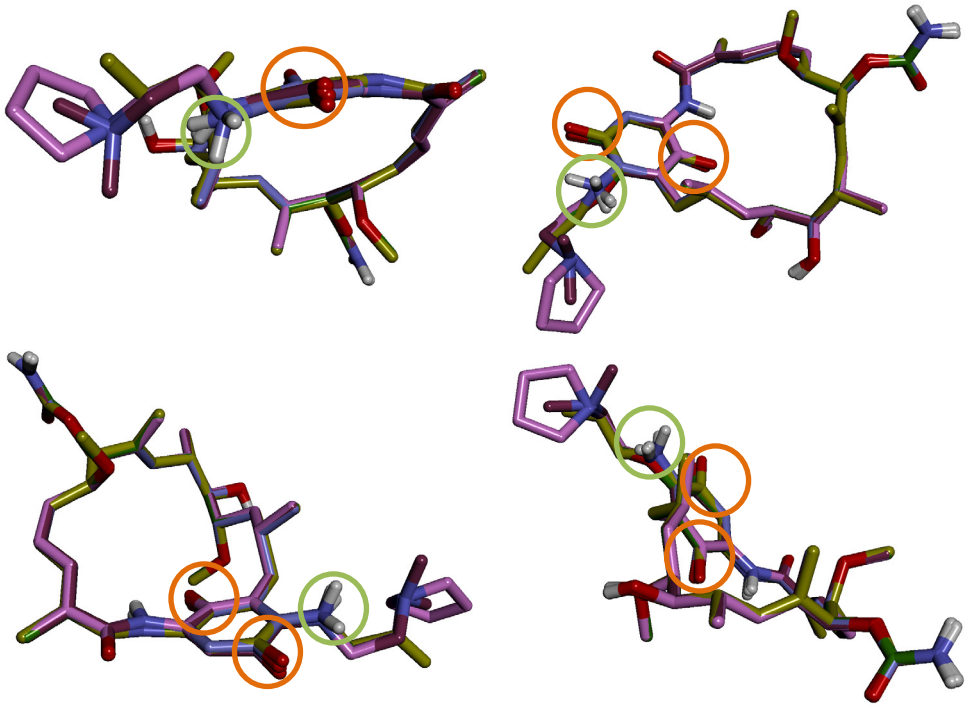

Figure 5.2. Molecular overlays of the benzoquinone ansamycins extracted from their respective docked complexes.

17AAG (carbon atoms colored yellow), GM (carbon atoms colored green), 17AG (carbon atoms colored lilac) 17DMAG (carbon atoms colored dark red), 17AEP-GA (carbon atoms colored pink).